CHALMERS TEKNISKA HÖGSKOLA

Institutionen för
Tillämpad termodynamik och strömningslära

CHALMERS UNIVERSITY OF TECHNOLOGY

Department of Applied Thermodynamics
and Fluid Mechanics

EFFECTS OF REYNOLDS NUMBER AND A LOW-INTENSITY FREESTREAM TURBULENCE ON THE FLOW AROUND A CIRCULAR CYLINDER

By

Christoffer Norberg

Göteborg Maj 1987

CONTENTS

SUMMARY

This paper presents experimental results from measurements on circular cylinders of different diameters in cross flow. The Reynolds number was varied from about 50 to $2 \cdot 10^5$. The combined effects of Reynolds number and a low-intensity freestream turbulence (Tu =1.4%) on the variation of different coefficients, e.g., Strouhal number, mean and RMS pressure coefficients, are presented. The results indicate that the flow is rather insensitive to an increase in the turbulence intensity at Reynolds numbers less than about 10^3. In this investigation, this is probably due to the large relative scales of the freestream turbulence at these Reynolds numbers (quasi-stationary flow). At higher Reynolds numbers (greater than about 10^3), the influence of turbulence is significant, especially concerning the pressure forces on the cylinder. It was found that the flow seems to exhibit a basic change at a Reynolds number of about $5 \cdot 10^3$ ($4 \cdot 10^3$ with turbulence). For instance, the relative Strouhal bandwidth changes by about one order of magnitude around this Reynolds number. A sub-division of the subcritical regime at this Reynolds number is proposed.

INTRODUCTION

The observation by Strouhal in 1878 [1], that the frequency (f) of the Aeolian tone [2] produced by his hand-driven whirler was proportional to the relative air velocity (U) and inversely proportional to the wire diameter (D) marks the beginning of the scientific study of the vortex shedding phenomenon. In 1908, Bénard [3] demonstrated that the periodic phenomenon was associated with a staggered vortex street formed behind the cylinder and the stability of the vortex configuration was investigated in a theoretical study by von Kármán [4] in 1912. That the dimensionless group fD/U, later called the Strouhal number [5], actually is a function of the Reynolds number was pointed out by Lord Rayleigh, in 1915 [6].

Here and in the following, the Reynolds number (Re = U_o D/v) is defined on the diameter of the cylinder (D), the freestream velocity (U_o) and the kinematic viscosity of the fluid (v).

The flow past a circular cylinder displays a series of flow regimes when going from low to high Reynolds numbers. When comparing different sources it should be remembered that the flow has been shown to be sensitive to disturbances and in particular to conditions at the end of the cylinder and to freestream turbulence [7-11]. At a Reynolds number of about 5 the flow behind the cylinder exhibits two symmetrical standing eddies [12]. With increasing Reynolds number the separated region elongates in the streamwise direction and when the "bubble length" is about two diameters [13], a wake instability occurs and the wake starts to "wobble" in a sinusoidal manner. Experiments on the determination of the upper limit of wake stability indicate a critical Reynolds number of about 34-40 [12-15]. From Re = 50 to about 150-200, the so-called stable regime [16], a stable laminar vortex street is generated [15, 16] (eventually the wake becomes unstable far downstream [17]). Evidence of different modes of laminar motion within the "stable" regime has been put forward by Tritton [18], Berger [19], Gerrard [13] and more recently by Sreenivasan [20]. It should be noted that some of these apparent changes might be due to some "non-uniformity in the flow" [21], end effects [7] or vibration of the cylinder [22].

With increasing Re, irregular disturbances in the vicinity of the vortex formation region [13, 23] appear at Re = 150-200. This marks the beginning of the transition regime [16]. It has been suggested [13, 23] that a three-dimensional distortion of the initially straight vortex lines eventually leads to turbulence in this regime. More regular vortex shedding reappears at Re ≈ 300-400. Above Re ≈ 300-400, the so-called subcritical regime, the transition to turbulence occurs before the separated layers roll up, the vortices once formed being turbulent [23]. In

this regime, the transition to turbulence is preceded by sinusoidal oscillations that appear in the separated shear layers. Bloor [23], who first discovered this phenomenon, associated it with "transition waves" and showed that (i) the ratio of transition wave frequency to fundamental frequency increased approximately proportional to the square root of the Reynolds number, (ii) the transition moves upstream with increasing Reynolds number (the transition has almost reached the shoulder of the cylinder at $Re = 5 \cdot 10^4$) and (iii) the formation region increases up to a maximum of about 3 diameters behind the cylinder axis as Re increases from about 400 to 1300 and it then decreases with increasing Re (the wake being formed about one diameter behind the cylinder axis at $Re \approx 5 \cdot 10^4$). A recent investigation by Wei and Smith [24] indicates that the "transition waves" detected by Bloor is identical to three-dimensional structures called "secondary vortices". It is suggested that the three-dimensional distortion of these vortices that follows immediately after their formation may provide the mechanism for the transition to turbulent Strouhal (fundamental) vortices. It has recently been shown; see Blevins [25]; that the vortex shedding in the upper subcritical regime consists of coherent strings of events whose frequencies wander about the nominal shedding frequency. When the transition occurs immediately after separation the flow will exhibit a high potential for reattachment. The so- called precritical regime with a steep fall in the drag coefficient with increasing Re begins at a Reynolds number of about $2 \cdot 10^5$ (dependent on surface roughness, free stream turbulence etc.). In the so-called paracritical regime with laminar separation, reattachment and, subsequently, turbulent separation only weak vortex shedding occurs. Reappearance of strong periodicity in the wake is found for Re greater than about $3 \cdot 10^6$. For a more complete discussion on different flow regimes, the reader is referred to e.g. [11, 26-29].

The data in this paper will be restricted to Reynolds numbers ranging from $Re \approx 50$ to about $2 \cdot 10^5$. Special attention will be given to the Reynolds number range between say $2 \cdot 10^3$ and 10^4 (i.e. within the "disturbance-sensitive Reynolds number range" [10]) and to the effects of a low-intensity freestream turbulence.

The given results complement an earlier paper [30].

EXPERIMENTAL ARRANGEMENT AND INSTRUMENTATION

The experiments were carried out in a closed-circuit low-speed wind tunnel, see Fig. l.
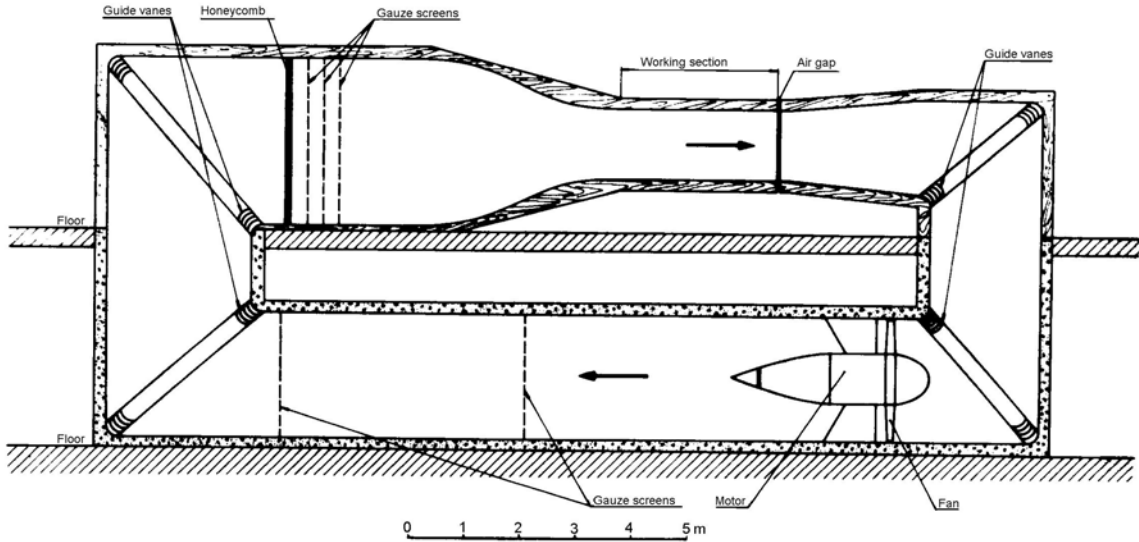

Fig. 1 The wind tunnel.

The settling chamber contains a honeycomb and three gauze screens and is followed by a 6:1 contraction into a 2.9 m long, 1.25 m high and 1.80 m wide test section. The corner fillets of 0.3 x 0.3 m^2 are somewhat diminishing in the flow direction in order to compensate for boundary layer growth. Effects of freestream turbulence could be studied by inserting a grid at the entrance of the test section. The grid was of bi-planar type with square meshes and circular rods (mesh size = 14.2 mm, bar diameter = 4 mm). The cylinders used in the experiments were all mounted horizontally with their axes perpendicular to the flow and at a position half-way between the roof and the floor and 1.5 m downstream of the grid centre plane. At this position, with the grid, the turbulence intensity was 1.35-1.39% and the eddy size (Λ) 11.3-12.1 mm in the velocity range 7-27 m/s [30]. The turbulence intensity without any grid was less than 0.06% in the velocity range 2-35 m/s. In the following, the cases with and without grid will be referred to as having Tu = 1.4% and 0.1%, respectively. The diameters of the cylinders used in the experiments varied from 0.251 to 120.0 mm, see Table 1.

Table 1   Data for cylinders of different diameters D.

L/D – Length between end plates to diameter
$\Delta A/A_o$ - Model blockage ratio, $A_o = 2.09$ m^2
D/H - Wall blockage ratio, H = 1250 mm
Λ - Longitudinal integral length scale

D [mm]	L/D	$\Delta A/A_o$	D/H	Λ/D	REMARK
0.251	1912	0.9	0.02	~50	Solid (music wire)
0.503	954	0.9	0.04	~25	Solid (-- " --)
2.00	240	1.0	0.2	~6	Solid (steel rod)
3.99	120	1.0	0.3	~3	Solid (-- " --)
5.98	80	1.0	0.5	2.0	Hollow
9.99	48	1.1	0.8	1.2	Solid (steel rod)
20.0	24	1.4	1.6	0.6	Solid/Hollow, see [32]
41.0	11.7	4.0	3.3	0.3	Solid/Hollow, see [31]
120.0	8.83	10.8	9.6	0.1	Hollow, see [30]

The mounting arrangement with end plates separated 480 mm (L) apart, originally designed for the cylinder having D = 41 mm [31], was used for all cylinders except for the one with D = 120 mm (see [30] for details on this cylinder). Both mean and fluctuating pressures could be measured with the cylinders having 20, 41 and 120 mm, see [30-32]. A pressure tap of 0.4 mm diameter was drilled, at the mid-span position, through the 0.4 mm thick wall of the cylinder with D = 5.98 mm (referred to as D = 6 mm). The rotation of the cylinder about its axis (with a rod from outside the tunnel) enabled the measurement of mean pressures around the perimeter. The angle from the stagnation point (α) was determined from the symmetry in the mean pressure distributions to an accuracy of about 1°. The cylinders with D = 2, 4 and 10 mm were smoothly machined steel rods with diameter tolerances of about 0.002 mm. The music wires (D = 0.25 and 0.50 mm) were stretched across the test section through holes in the side walls and then clamped to the passages through the end plates. The diameters of the music wires were measured with a microscope (Leitz Wetzlar) to an accuracy of about 2 μm. The diameters of the cylinders with D = 2, 4 and 10 mm were calibrated against standard reference lengths (C. E. Johansson).

The passages through the end plates were sealed to prevent leakage flow. Care was taken in order to align the cylinders perpendicular to the mean flow direction.

The freestream velocity (U_o) was measured with a Pitot-static tube (United Sensor) positioned 0.77 m downstream of the grid centre-plane. The pressure differences for velocity determination were read on a liquid manometer ($U_o > \sim 5$ m/s) to an accuracy of about 0.02 mm alcohol or measured with a micromanometer (Furness Control Ltd.) to an accuracy of about 1% (1.5 m/s $< U_o < \sim 5$ m/s). The overall relative error in the determination of the freestream velocity was estimated to be < 0.5% for velocities greater than 5 m/s and < 1% for velocities less than 5 m/s. The micromanometer was employed in the measurements of mean pressures around the cylinders. The reference pressure in the determination of the mean pressure coefficients (C_P) was taken as the static pressure from the Pitot-static tube.

In the wake surveys the hot wire (Dantec P05) and its support were mounted on a wing-shaped profile standing on a coordinate table and a vertical mechanism grounded to the floor. In the correlation studies the wing-shaped profile was omitted and hot wires of a smaller size (Dantec P15) were used. The computed cross-correlation coefficients were based on 256 to 512 ksamples at each point of measuring. The origin of the coordinate system used is on the cylinder axis mid-way between the end plates; x denotes the oncoming flow direction and y the direction normal to the cylinder axis (downwards), see Fig. 2.

The shedding frequency (f_S) was calculated from the frequency given by the arithmetic mean of the two frequencies where the spectral level was 3 dB lower than the peak value in the calculated spectra. The difference between the two frequencies (Δf_S) was used as a measure of the bandwidth of the peak. The analysing bandwidth was about 0.3% of the shedding frequency for diameters up to 10 mm and about 0.2 Hz for D = 41 and 120 mm.

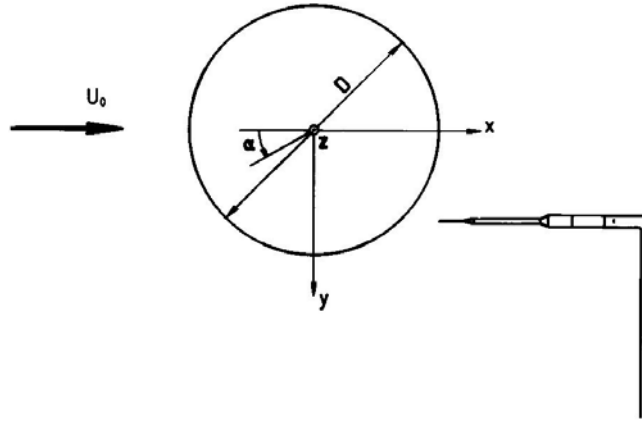Further details on experimental arrangements and instrumentation can be found in [30].

Fig. 2 Coordinate system.

RESULTS AND DISCUSSION

The first part deals with the variation of the Strouhal number with Reynolds number at the two freestream conditions (Tu = 0.1% and 1.4%). The different flow regimes are discussed. After that, some results on the transition frequency and its relation to the fundamental frequency are presented. The following part is concentrated on the variations in the Reynolds number range between $2 \cdot 10^3$ to 10^4. In this range a fundamental change in the vortex shedding process seems to occur. A comparison between four cases in this range is presented. Results on the vortex formation distance as well as correlations in the axial (spanwise) direction are given. Finally, some results on the Reynolds number dependence and the influence of a low-intensity turbulence intensity on the mean- and RMS pressure coefficients at the base are given.

STROUHAL NUMBER

Presentation of results

A very large amount of experimental information is available on the flow around a circular cylinder. However, when collecting data from different investigations and then putting them together it is apparent that many factors have an influence on the flow. The Reynolds number is of course an important parameter but the flow is also sensitive to factors that describe e.g. freestream turbulence, surface roughness, blockage and end conditions. One important quantity that is easily measured is the vortex shedding frequency. The Strouhal number is defined as:

$$St = f_S D/U_o$$

where f_S - vortex shedding frequency, D - cylinder diameter and U_o freestream velocity. In Fig. 3, the Strouhal number and the relative bandwidth of the Strouhal peak at the two turbulence intensities (Tu = 0.1% and 1.4%) are plotted against the Reynolds number. The data points that are compiled in Fig. 3 are given in the Appendix. The Strouhal numbers for the cylinders with diameters of 41 and 120 mm have been given in an earlier paper [30] but they are included for the sake of completeness. The freestream velocities for the largest cylinder (D = 120 mm) were corrected 5.8% in order to compensate for the effect of blockage (see [30]). No blockage correction was applied for the other cylinders. The relative bandwidth ($\Delta f_S/f_S$) can be seen as a measure of the sharpness of peak at the vortex shedding frequency in the power spectral density. The variations of the Strouhal number at Reynolds numbers less than 1000 and greater than 2000 and the effect of the turbulence intensity are shown in Fig. 4.

Fig. 3a Strouhal number vs Reynolds number for Tu = 0.1%. Freestream velocity for D = 120 mm corrected for blockage (5.8%).
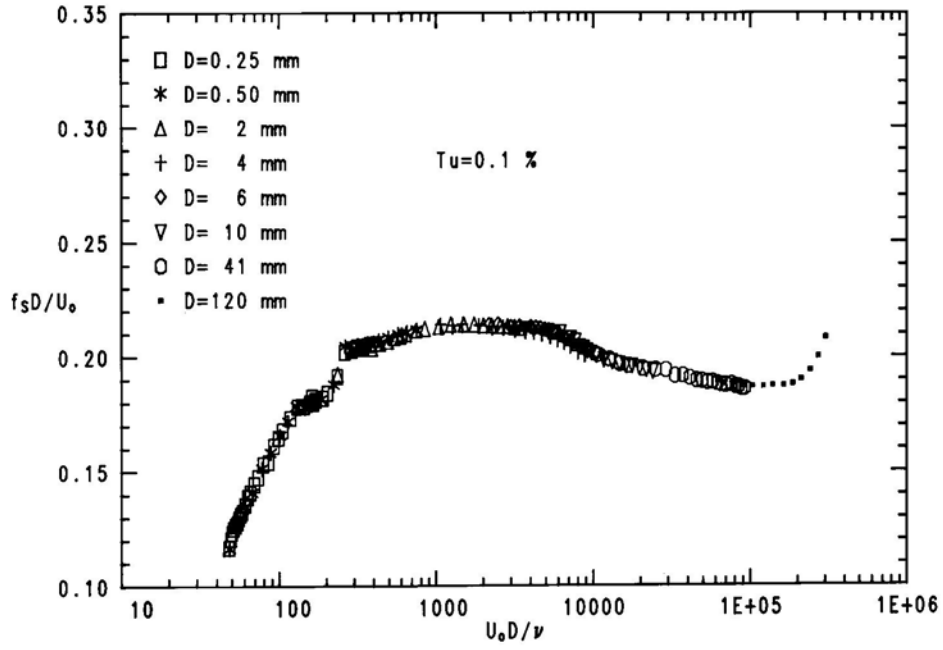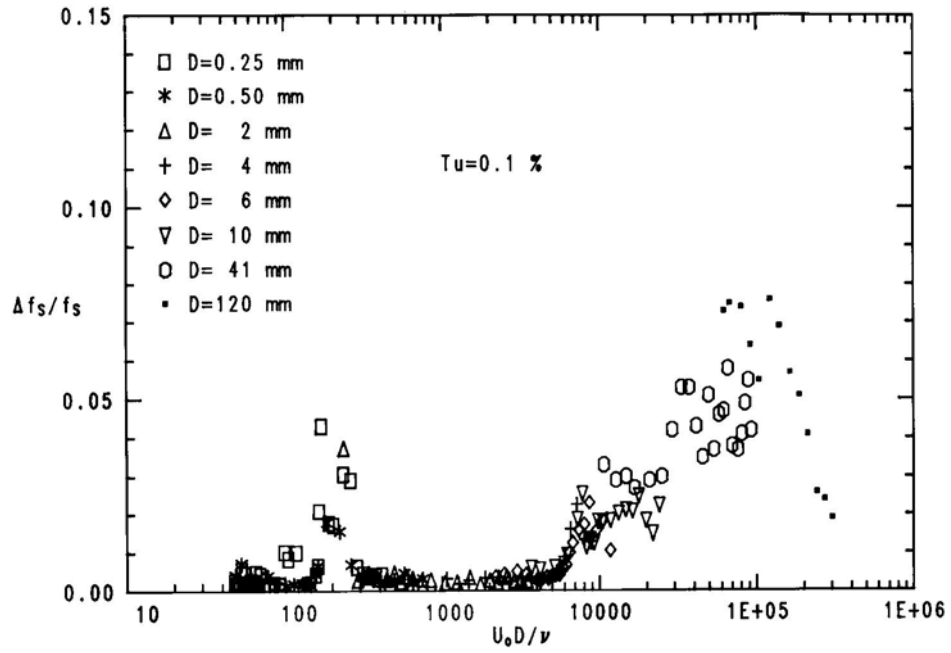

Fig. 3b Relative bandwidth of Strouhal peak vs Reynolds number for Tu = 0.1%. Freestream velocity for D = 120 mm corrected for blockage (5.8%).
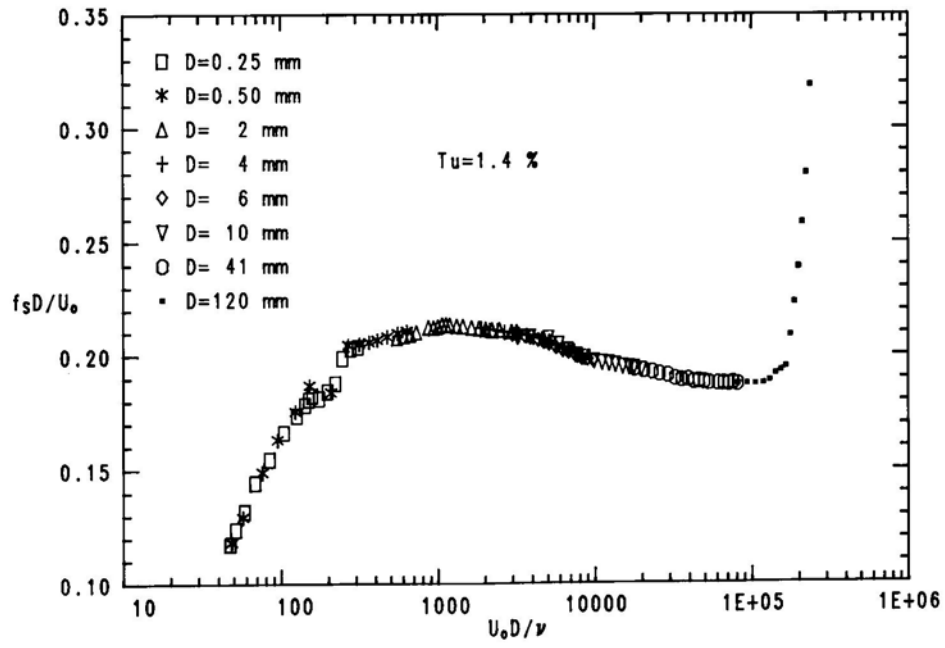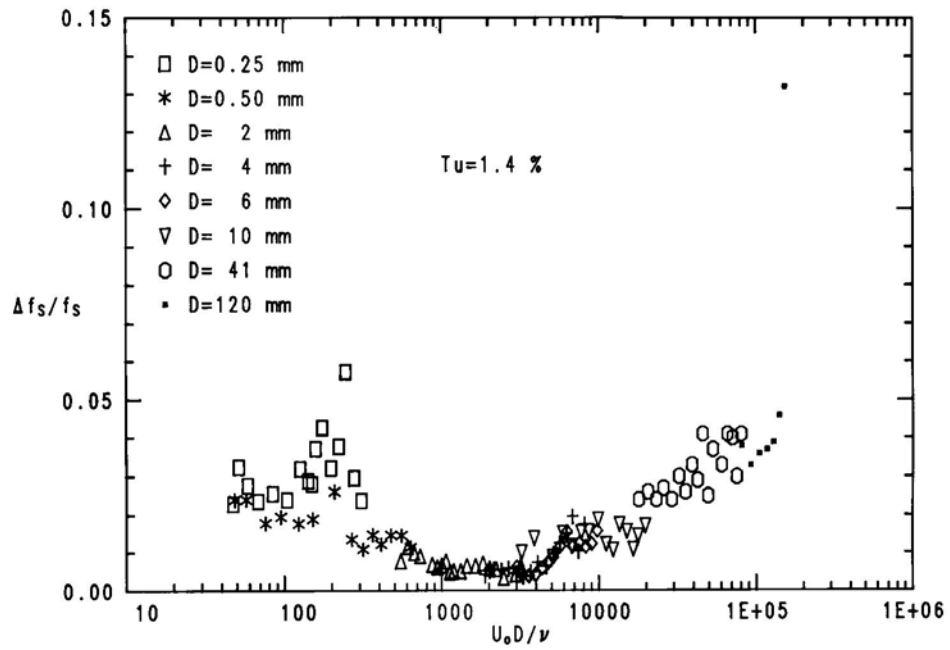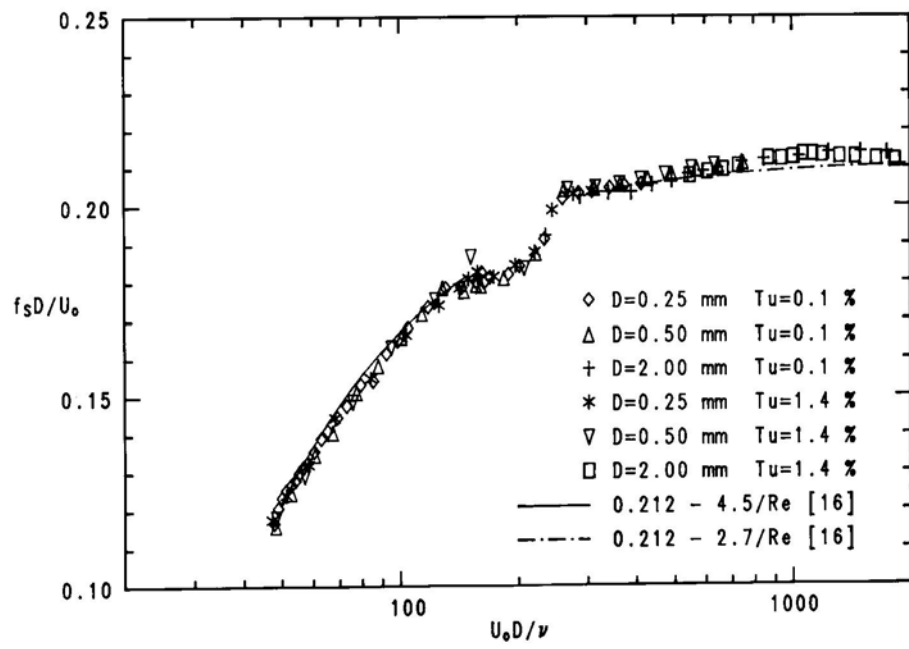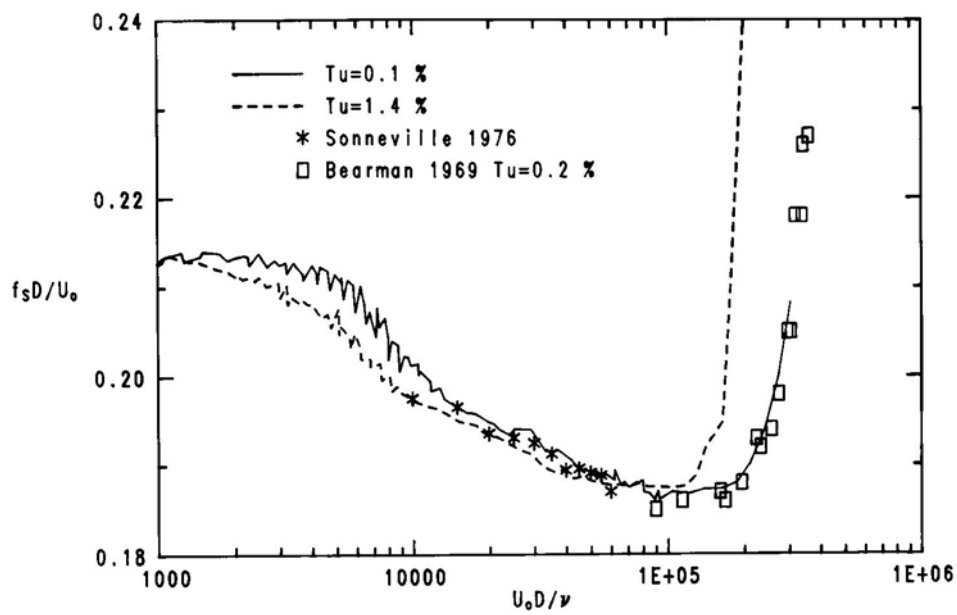
Fig. 3c   Same as Fig. 3a, except Tu = 1.4%.

Fig. 3d   Same as Fig. 3b, except Tu = 1.4%.

11

Fig. 4   Strouhal number vs Reynolds number.
          (a) Re less than 2000, (b) Re greater than 1000.

Accuracy

The maximum relative error in the determination of the Strouhal number can be estimated as:

$$\left| \Delta St/St \right|_{max} = \left| \Delta f_S/f_S \right|_{max} + \left| \Delta D/D \right|_{max} + \left| \Delta U_o/U_o \right|_{max}$$

With the accuracy of the given quantities, as given earlier, the relative error is less than 2.5%. This value is a conservative estimate, which includes random as well as fixed (systematic) errors. The results for the different diameters, in the overlapping regions, show an excellent continuity. Thus, it can be expected that the fixed errors are very small. As judged from the scatter of the data, the random errors also seem to be small (less than 1%). Thus a more realistic estimate of the accuracy of the given Strouhal numbers is about 1.5% (total relative error). It should be noted that the accuracy of the Strouhal frequency is determined from the analysing bandwidth and not from the relative bandwidth of the Strouhal peak (which amounts to several percent in some cases with a relative large scatter).

End conditions and vibration

All measurements of the Strouhal frequency in this investigation were made at the mid-span position. The importance of end conditions has been pointed out by Gerich and Eckelmann [7]. They concentrated on the flow at Reynolds numbers less than about 250 and found that the cylinder end boundaries, whether they are end plates or simple free ends, alter the vortex shedding near the boundaries. In the boundary-affected regions (6 to 15 diameters in length) the Strouhal number was found to be 10-15% less than in the unaffected regions. Based on the results given by Gerich and Eckelmann and available data on axial correlation lengths (see e.g. [33]), the present aspect ratios are considered to be sufficiently large. Also the use of end plates of proper design [8] is expected to improve the end conditions.

The Strouhal number for a vibrating cylinder, due to lock-in [34], is lower than the corresponding value for a stationary cylinder. Only for the cylinders having D = 6 and 10 mm, the calculated first and second mode natural frequencies were in coincidence with the shedding frequencies. No evidence of any synchronisation behaviour was observed in these cases. For the cylinders with diameters up to 4 mm the first and second mode natural frequencies were much lower than the shedding frequencies. Aeroelastic coupling of the

vortex wake with vibration modes of high order has recently been observed by Van Atta and Gharib [22] (Re less than 160). As discussed further below, the frequency measurements with the music wires (D = 0.25 and 0.50 mm) indicated a very slight wake-cylinder coupling at some occasional velocities. Nevertheless, it is believed that the present data truly represent the case with a stationary cylinder.

Onset of vortex shedding

The critical Reynolds number, Re_c, at which the vortex shedding started (i.e. the onset value for periodic shedding) was about 48 the onset value of the Strouhal number being about 0.117, see Figs. 3 and 4a. There was no effect on Re_c within the experimental accuracy, from the different flow conditions. It is interesting to note that Camichel et al. [35], in a visualization study dating back to 1927, found more or less the same critical values as in this study (Re_c = 47-48, St = 0.117). Kovásznay [15] found a critical value of 40 and he also noted that the transition did not have any hysteresis. That the critical value was the same for increasing and decreasing velocities was also observed in this investigation. Nishioka and Sato [36] have shown that the critical Reynolds number increases with decreasing aspect ratio and they found that $Re_c \approx 48$ for aspect ratios greater than about 40. The hot wire measurements by Kohan and Schwarz [37] and Friehe [38] also indicated a critical Reynolds number of about 50. Water visualizations by e.g. Taneda [39] and Gerrard [13] show that the wake begins to oscillate far downstream in a sinusoidal fashion at a Reynolds number of about 30-34 and that the alternate shedding starts at Re $\approx$ 45-55. The shedding seemed to be initiated by elongations of the gathers that appear in the twin vortices behind the cylinder. Tritton [15] denoted this type of shedding the "low-speed mode".

Transitions in the stable regime?

Tritton observed a sudden decrease in the Strouhal number at a Reynolds number of about 90. A visualization indicated that this "irregularity" was connected to a shift into a mode in which the shedding came directly from the cylinder and he denoted this type of shedding the "high-speed mode". Berger [19] later confirmed the findings by Tritton. Gaster [21], however, did not observe any "Tritton jumps" in his frequency measurements with a circular cylinder. In his experiments with tapered cylinders having a circular cross section and later [40] with a circular cylinder in non-uniform flow he found discontinuities like those observed by Tritton.

This lead him to the conclusion that non-uniformities in the oncoming flow are responsible for the observations of the different flow modes. Tritton then repeated his measurements using another apparatus [41]. He then again observed a discontinuity but now at a higher Reynolds number (Re = 110). Transitions around a Reynolds number of 100 have been observed in other investigations, see e.g. [13, 20, 36]. Gerrard [13] suggested that the decrease in the base pressure coefficient around Re = 100 (see [11]) corresponds to an increase in the flow motions in the base region and that this is an indication of that convection becomes dominating over diffusion. Friehe [38] presented continuous recordings of the vortex shedding frequency versus freestream velocity for a number of diameters in different flow conditions. He found several "Tritton jumps" at different Re in the Reynolds number range 50 to 180. He noticed that in some cases the "jumps" were very small and therefore hard to detect from the variations in the shedding frequency.

Within the experimental accuracy, the present Strouhal numbers are seen to vary continuously with Reynolds number in the stable regime (Re less than about 160) and therefore no conclusion about the presence of any "jumps" can be drawn, see Figs. 3 and 4a.

In the frequency measurements with the cylinders having D = 0.25 and 0.50 mm the hot wire was situated at $x/D \approx 10$, $y/D \approx 3.3$. At this position the velocity variations in the stable regime, with no additional turbulence, were regular and it was often very difficult to distinguish the hot wire signal from the signal from a sine-wave generator. Occasionally and only at certain velocities, the steady regular motion seemed to be slightly disturbed. Lissajous-figures observed on an oscilloscope showed in these cases a somewhat "shaky" appearance and a closer examination of the spectral density of the velocity fluctuations, see e.g. Fig. 5, revealed a two-frequency behaviour.
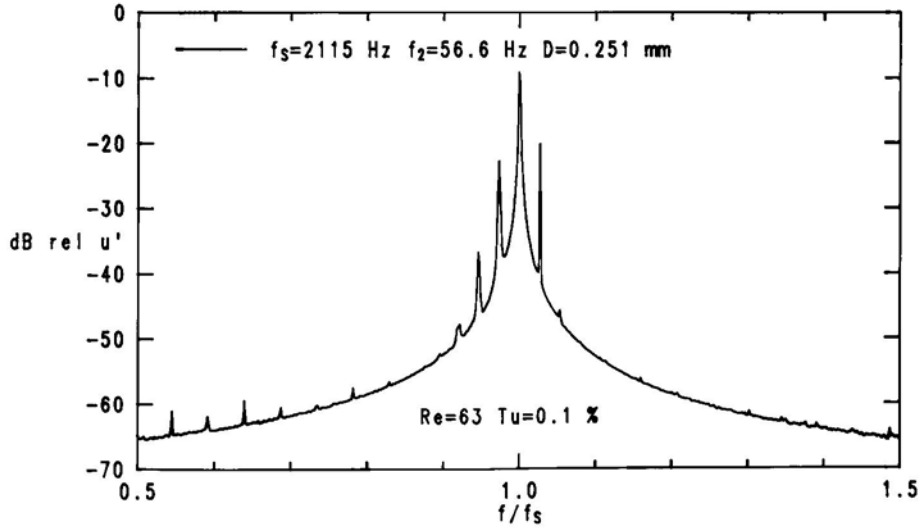
Fig. 5 Spectra of velocity fluctuations in the wake at Re = 63 showing a two-frequency
(f_S, f_2) behaviour.

Apart from peaks at the additional frequency f_2 and its harmonies simple combinations of the
basic shedding frequency f_S and f_2 could be identified (in Fig. 5 peaks at f_S-$3f_2$, f_S-$2f_2$, f_S-f_2,
(f_S), f_S+f_2, f_S+$2f_2$ are clearly visible).

The hot wire measurements by Sreenivasan [20] in the wake of a circular cylinder at low
Reynolds numbers showed in the sense of the theory of Ruelle, Takens and Newhouse [42],
the so called "RTN scenario", "aspects of similarity with low-dimensional chaotic dynamical
systems". One important feature in this description is the alternation between regions of
"order and chaos" appearing with increasing Reynolds numbers. "Quasiperiodicity" with up
to four independent frequencies appeared in the ordered regions in the "stable" regime.
Regions of "chaos" occurred approximately in the intervals Re = 66-71, 81-90 and 140-143.
A so-called "rotation number", defined as the ratio between an extra frequency to the
fundamental shedding frequency, was introduced. Sirovich [43] performed a modal analysis
of different perturbation modes of oscillations of the classical "Karman vortex street" and he
found reasonable agreement with the experimental rotation numbers given by Sreenivasan.
Despite the extensive cover of the stable regime, especially with the cylinder with D = 0.25
mm and Tu = 0.1%, no evidence of a "chaotic" behaviour as described by Sreenivasan was
found. A characteristic feature for the "windows of chaos" seems to be a substantial
broadening of the fundamental peak. The relative bandwidths in the chaotic regions of
Sreenivasan were of the order 100 times the ones found in the ordered regions. As seen in
Fig. 3, no similar variations can be found. The two-frequency behaviour was only noticed
with no additional turbulence (Tu = 0.1%). With the 0.25 mm wire, two frequencies were

16

clearly distinctable at Re = 63 (see Fig. 5) and at Re = 131, the corresponding rotation numbers being 0.027 and 0.020, respectively. With the 0.5 mm wire one additional frequency was present at Re = 101 and 156 (f_2/f_S = 0.023 and 0.054, respectively). The rotation numbers of Sreenivasan (given in [43]) show an increase with Reynolds number from about 0.03 at Re = 50 to about 0.08 at Re = 110. Thus it seems that only the ratio of 0.027 at Re = 63 (Fig. 5) compares favourable with the data of Sreenivasan. It is interesting to note that the data of Sreenivasan shows breaks in the variation of the shedding frequency with Reynolds number in coincidence with the windows of chaos. Similar breaks and "windows of chaos" were apparently not present in this study. The recent paper by Van Atta and Gharib [22] has shown that the appearance of additional frequencies and regions of "chaos" have a clear connection to an aeroelastic coupling to excited cylinder vibration modes. The additional frequencies that were found in the measurements by Van Atta and Gharib, at Reynolds numbers less than 160, were all simply related to the natural frequencies of the cylinder. The broadening of the fundamental peaks in the "windows of chaos" was found to be due to switching between different competing coupling modes of vibration. Varying the damping of the wires could easily change the nature and degree of the aeroelastic coupling. They also found that the Reynolds numbers at the locations of discontinuities varied as the tension (i.e. natural frequency) was varied. The measurements by Van Atta and Gharib suggest that the Strouhal-Reynolds number variation, in the Reynolds number range considered, would have no discontinuities if there were absolutely no vibration of the cylinder.

The additional frequencies for the 0.25 mm wire were 56.6 Hz and 113.2 Hz (113.2/56.6 ≈ 2) while the additional frequencies observed with the 0.50 mm wire were 23.1 Hz and 91.6 Hz (91.6/23.1 ≈ 4). The near integer values of the ratios support the explanation of aeroelastic coupling given by Van Atta and Gharib. Unfortunately, the natural frequencies of the stretched music wires were not measured directly. Nevertheless, a rough calculation, taking the approximate tension applied into account, indicated that the fundamental vibration frequencies were of the same order as the lowest additional frequencies (i.e. 20-60 Hz). The fact that aeroelastic coupling is a source to irregularities in the Strouhal-Reynolds number relation puts a question to whether real transitions actually occur in the flow around a stationary cylinder in the stable regime. Further measurements and theoretical achievements are needed in order to clarify this matter.

It is important to note that the Strouhal numbers for Reynolds numbers less than about 1000, see Fig. 4a, were unaffected by the presence of a low-intensity freestream turbulence. Thus it must be concluded that due to the relatively large scales of the freestream turbulence at these Reynolds numbers (see Table 1) the vortex shedding frequency varies in accordance with a quasi-stationary process. If this is correct the variations in the vortex shedding frequency would produce a relative bandwidth of the Strouhal peak proportional to the freestream turbulence intensity divided by the mean Strouhal number. Apart from the increase in the relative bandwidth in the transition regime (Re = 160 - 260), see Fig. 3, this seems to be the case. Hussain and Ramjee [41] also noticed that freestream turbulence of moderate levels (Tu = 0.3-8%, $\Lambda/D \approx$ 2-10) not affected the shedding frequency. It is important to point out that the freestream turbulence might change the Strouhal number at other scales and intensities.

Proposals for Re-dependence at low Re

There exists a number of investigations on the Reynolds number - Strouhal number relation. Table 2 summarizes some of the proposals of the relationship. They are on the form:

$$St = A - B/Re + C \cdot Re$$

Table 2   Comparison of different expressions giving the Strouhal number as
           $St = A - B/Re + C \cdot Re$

No	Author(s)	A	B	C	Limits Re	Ref.
1	Roshko (1954)	0.212	4.5	0	50-150	[16]
2	-- ” --	0.212	2.7	0	300-2000	[16]
3	Tritton (1959)	0.144	2.1	$4.1 \cdot 10^{-4}$	50-105	[18]
4	-- ” --	0.224	6.70	0	80-150	[18]
5	Berger (1964)	0.197	3.93	0	50-105	[19]
6	-- ” --	0.164	2.55	$1.625 \cdot 10^{-4}$	50-170	[45]
7	-- ” --	0.224	6.70	0	115-135	[19]
8	-- ” --	0.220	7.4	0	130-160	[19]
9	Kohan/Schwarz (1973)	0.19	3.57	0	40-75	[37]
10	-- ” --	0.216	5.77	0	90-130	[37]
11	-- ” --	0.19	2.60	0	130-160	[37]
12	Gerrard (1978)	0.1959	3.811	0	41-93	[13]
13	-- ” --	0.2064	5.173	0	101-256	[13]
14	-- ” --	0.1913	-2.791	0	380-767	[13]
15	Present	0.211	4.6	0	50-150	
16	-- ” --	0.215	3.4	0	300-2000	

The Strouhal numbers given by Roshko [16] were measured in an air stream having a turbulence intensity of about 0.03%. Roshko found for the stable regime A = 0.212 and B = 4.5 (Re = 50-150). As seen in Fig. 4a, the deviations from this relation are very small. In fact, a least square analysis to the data in this range (40 data points) gave A = 0.211 and B = 4.6 with a RMS deviation in the Strouhal number of about 1%. Thus, the present data is a support for the "Roshko relation" in the stable regime (number 1 in Table 1). It is worth noting that the Strouhal numbers reported by Gerich and Eckelmann [7] in the unaffected regions (stable regime) were close to the Roshko relation. Also the relation given by Tritton [18] in the Reynolds number range from 50 to 105 (number 3 in Table 2) compares well with the present data. However, some of the relations in Table 1 show noticeable deviations. For instance the relation given by Berger [19] for the so-called "basic mode" (number 8 in Table 2) and the relation given by Gerrard valid at Reynolds numbers in the range 380 to 767 (number 14)

gave Strouhal numbers that were about 6% lower than the present data. Berger's relation was claimed to be valid for extremely low turbulence intensity in the free stream (Tu less than 0.05%). The deviation from Berger's relation cannot be explained unless the origin and perhaps the scale of the "turbulence" at these low intensities are completely different. Also the effect on the Strouhal numbers from vibrations at small amplitudes cannot be excluded in some of the earlier measurements. Van Atta and Gharib [22] noticed that the deviations from the "Roshko relation" (1) were small when there was absolutely no vibration of the cylinder. Bloor [23] noticed that the extent of the stable regime was increased when the freestream turbulence intensity was changed from about 1% to 0.03%. Berger and Wille [26] suggested that the different Strouhal - Reynolds number relations (see Table 2) are due to different turbulence intensities in the oncoming flow. The present results (Tu = 0.1-1.4%) do not support this explanation. The experiments by Gerrard were performed with cylinders towed in still water. In this case the rather low aspect ratios used might explain the discrepancy (see Gerich and Eckelmann [7]).

Transition regime

It is generally recognized (see Berger and Wille [26]) that the transition regime extends from Re ≈ 150-200 to Re ≈ 300-400. As shown by Hama [46], a transverse waviness appears close behind the cylinder at the beginning of the transitional regime. According to Bloor [23], the transition to turbulence occurs after the vortices have rolled up, the transition mechanism being due to a three-dimensional distortion. Definite breaks in the Strouhal number variation occurred at Re ≈ 160 and at Re ≈ 265, see Fig. 4a. As seen in Fig. 3, these breaks are accompanied with significant changes in the relative bandwidths. It is assumed that these breaks distinguish the beginning and end of the transition regime. In the paper by Gerrard [13] the transition regime is discussed in more detail.

Subcritical regime

The visualizations by Gerrard [131 show that the flow in the Reynolds number range from about 250 to 500 changes to a mode of shedding which is similar to the "vortex formation model" as described by Gerrard in [47]. Gerrard [13] also noted that the instabilities of the shear layers preceding a transition to turbulence appear around Re = 350. The frequency of the "transition waves" (see Bloor [23]) or "secondary vortices" (see Wei and Smith [24]) is

discussed in the following section. It appears that a change in slope in the Strouhal number variation takes place at a Reynolds number of about 800, see Fig. 3. The significance of this change is uncertain and further measurements are needed in order to clarify this matter. Roshko [16] denoted the range of Reynolds number above the transition regime the "irregular range" and he proposed a relation for the Strouhal numbers valid from Re = 300 to 2000 (relation 2 in Table 2). From Fig. 4a, it can be seen that the deviations from this relation are small but that the present Strouhal numbers lie slightly above at Reynolds numbers greater than about 600. A least square fit to the present data gave the relation (16) given in Table 2 (50 points, RMS deviation 0.5%).

It is evident from Fig. 4b that the Strouhal number above Re ≈ 1000 is dependent on the turbulence intensity. The Strouhal numbers are lower at the higher turbulence intensity in the Reynolds number range from about 10^3 to 10^5 the difference being greatest at around Re = $5 \cdot 10^3$. The Strouhal bandwidths show a marked increase at around a Reynolds number that apparently is depending on the turbulence intensity. At Tu = 0.1% the increase starts at about Re = $5 \cdot 10^3$ while at Tu = 1.4% the same phenomenon occurs at about $4 \cdot 10^3$, see Fig. 3. Above these Reynolds numbers the Strouhal number decreases significantly. The high sensitivity to freestream disturbances in this range is reflected in the curve for Tu = 0.1% in Fig. 4b. The lower bound for this curve is due to the Strouhal numbers measured with the cylinder having D = 4 mm (see Fig. 3a). At these Reynolds numbers, it can be suspected that the freestream disturbance level was slightly higher at corresponding higher velocities than for the other diameters. The whole region between the end of the transition regime at Re ≈ 300 to the beginning of the critical regime at Re ≈ $2 \cdot 10^5$ (dependent on e.g. turbulence intensity) is often referred to as the subcritical regime [29]. In the following the subcritical regime will be sub-divided at about Re = $5 \cdot 10^3$ (Tu-dependent, see above) into a lower subcritical and an upper subcritical regime. As seen in Fig. 3, the relative bandwidths in the lower subcritical regime are much smaller than in the upper subcritical regime. It is noticeable that there seems to be a correlation between the increasing relative bandwidths and the increase in the mean and fluctuating forces on the cylinder in the upper subcritical regime, see [30]. In the Reynolds number range from 10^3 to 10^4 only a few Strouhal number measurements have been reported. The measurements by e.g. Roshko [16] are in a qualitative agreement with the present data. There is a favourable agreement between the present Strouhal numbers at Tu = 0.1% and the compatible measurements by Bearman [48] and Sonneville [49], see Fig. 4b. Further discussion on the variations in the subcritical regime will be given in a later section. It is

noticeable that the Strouhal bandwidths, see Figs. 3b and 3d, when entering the critical regime, show a decrease at Tu = 0.1% but an increase at Tu = 1.4%.

TRANSITION FREQUENCY

In Fig. 6, simultaneous velocity variations measured with two hot wires separated two diameters in the axial direction (Re = 5·10^3 Tu = 0.1%) are shown.
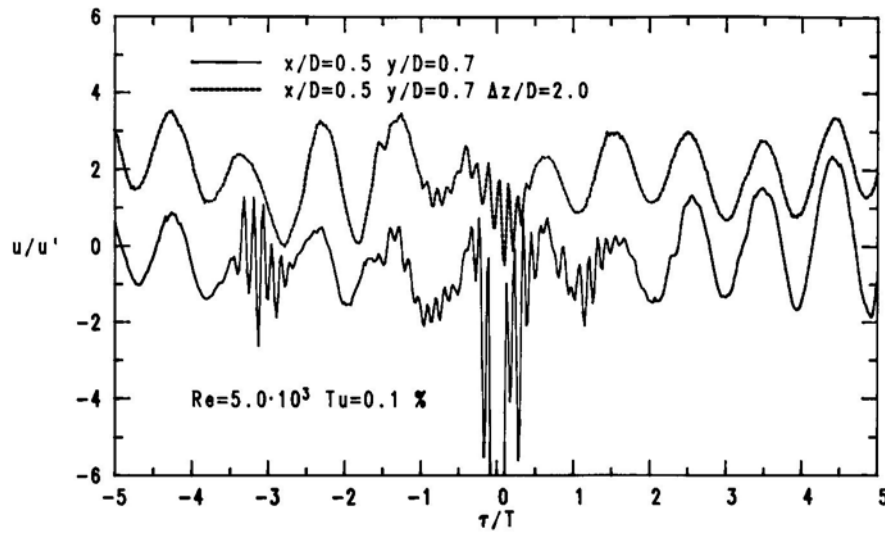
Fig. 6 Traces of velocity fluctuations measured with two hot wires separated two diameters apart in the axial direction. Note: upper trace displaced two RMS-units upwards.

Both hot wires were located at the relative position 0.5 diameters behind and 0.7 diameters below the cylinder axis (x/D = 0.5, y/D = 0.7, see Fig. 2). At this position, evidence of the so-called "transition waves" [23] or "secondary vortices" [24] are clearly recognized. By counting the number of oscillation periods the transition frequency can be estimated to be about 8 times the vortex shedding frequency in this case. However, the frequency of these oscillations is not so well defined as the vortex shedding frequency. The appearance and the frequency of the oscillations seem to vary from time to time. The broad-band nature of the shear layer oscillations can be seen in Fig. 7.
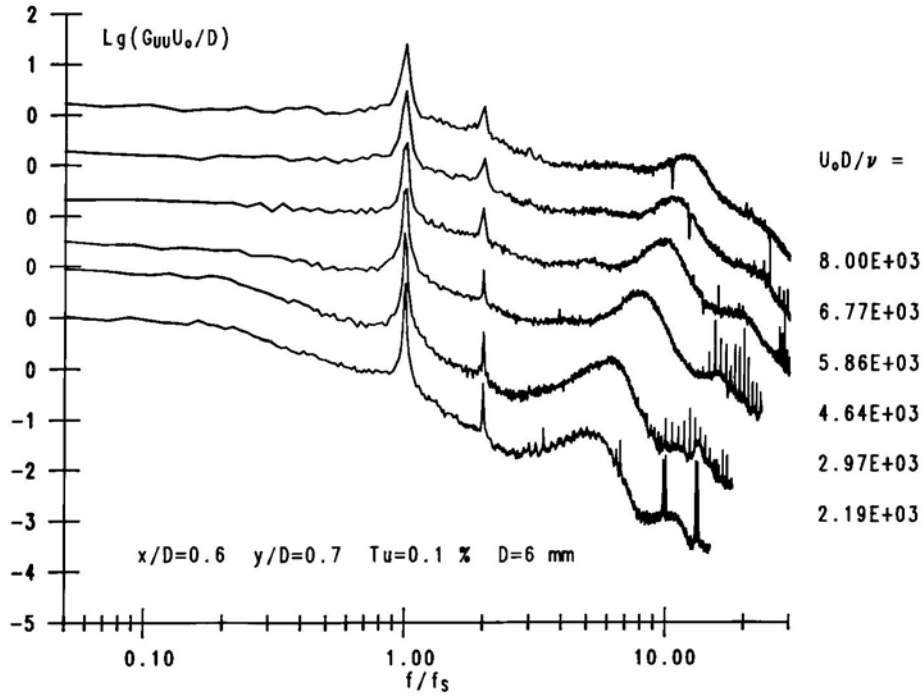
Fig. 7   Spectra of velocity fluctuations at x/D = 0.6, y/D = 0.7 for Tu = 0.1%, D = 6 mm.

It is evident from Fig. 7 that the ratio of the transition frequency to the shedding frequency increases with Reynolds number. The broadening of the peaks at f_S and $2 \cdot f_S$ when passing Re $= 5 \cdot 10^3$ is also evident from this figure. The center frequency of the shear layer oscillations (f_T) was determined in the same way as for the vortex shedding frequency (arithmetic mean between the two frequencies where the levels are 3 dB down from the peak value). The present measurements were restricted to the case with Tu = 0.1% (D = 6 and 41 mm) and the ratios found are shown in Fig. 8. With additional freestream turbulence the center frequencies were in some cases difficult to determine from the spectra. It was however noticed, in the cases in which it was possible, that the influence of the turbulence intensity was negligible (i.e. within the experimental accuracy).
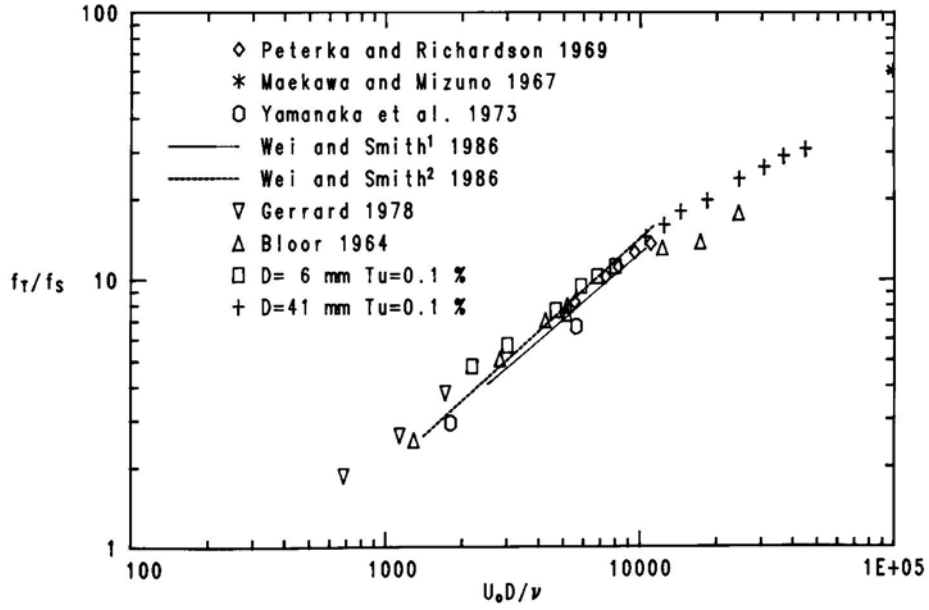
Fig. 8   Transition frequency to Strouhal frequency vs Reynolds number.
[1]Flow-visualization, [2]Hot wire data [24].

Bloor [23] found that the ratio f_T/f_S appeared to be proportional to the square root of the Reynolds number, i.e., $f_T/f_S \sim Re^{0.5}$. This relationship was justified by the following arguments: (i) transition frequency scales on the ratio between the freestream velocity and the boundary layer thickness; $f_T \sim U_o/\delta$, (ii) $\delta/D \sim Re^{0.5}$ (see e.g. [50]) and (iii) $f_S \sim U_o/D$ (Strouhal number relatively constant). The recent measurements by Wei and Smith [24] indicate, however, that f_T/f_S is proportional to a power of the Reynolds number greater than 0.5. They found a 0.87 power relation from flow-visualization observations and a 0.77 power relation from hot wire measurements, see Fig. 8. They also noted that a regression fit to the data points reported by Bloor [23], see Fig. 8, actually gave a 0.73 power relation. They argued that it was more reasonable to expect that the transition frequency should scale on the momentum thickness characteristic for the middle of the linear growth region of the shear layers. Unal and Rockwell [51] found, using this scaling, that the vortex formation, at least up to Re = 5040, was in accordance with linear stability theory [52]. In addition to the data presented in Fig. 8, Unal and Rockwell reported $f_T/f_S \approx 8$ at Re = 5040. The present ratios indicate that the exponent in a fitted power relation changes with Reynolds number; the increase (or exponent in a power relation) being greatest at Re $\sim 5 \cdot 10^3$. Extrapolating the present data, as given in Fig. 8, up to Re = 10^5 would give a ratio of about 40. This value is much lower than the value 60 reported by Maekawa and Mizuno [53] at this Reynolds number. The hot wire measurements by Peterka and Richardson [54] and later by Yamanaka

24

et al. [55] were concentrated on the high sensitivity to (acoustical) disturbances at frequencies around the transition frequency; a phenomenon which was first noticed by Gerrard [10]. Peterka and Richardson observed a sub-harmonic peak in the velocity spectra measured in the shear layer when the forcing was applied around the (natural) transition frequency. They did not observe any sub-harmonic peak with no forcing applied. Some evidence of a raised spectral level around a frequency at $f_T/2$ can be found in the spectra at the higher Re in Fig. 7. There is also evidence (perhaps more clear) of peaks at frequencies around $2 \cdot f_T$ (1st harmonic). The existence of sub-harmonics and harmonics may imply that the vortical structures interact in a non-linear way and according to Peterka and Richardson the most probable mechanism behind sub-harmonic peaks is vortex fusion. It is noticeable that no evidence of a non-linear coupling between the vortex shedding frequency and the transition frequency are seen in the spectra. Interactions between the "secondary vortices" and the fundamental vortices as well as feedback mechanisms between the "secondary vortices" were observed by Wei and Smith [24]. Wei and Smith hypothesized that the initial development of the "secondary vortices" is due to a three-dimensional distortion of an initially straight line vortex filament in a way similar to the mechanism described by Hama [56]. It is quite remarkable that similar interactions as some of those observed by Wei and Smith, which apparently have strong three-dimensional ingredients, were observed in the numerical study by Braza et al. [57] (two-dimensional computation). Gerrard [13] observed that the "transition waves" were in phase on the two sides of the wake but also in phase along the length of the cylinder. However, the evidence (flow-visualization) for the phase-match in the spanwise direction was not totally convincing (at least not to the author of this paper!). The flow-visualizations by Wei and Smith [24], see also [58], show the existence of "axial vortex pairs" or "spanwise pockets" [58] whose extent in the axial direction decreased with increasing Re. It is reasonable to believe that the coupling of these structures in the axial direction also decreases with increasing Re. The measurements with two hot wires separated in the axial direction, see Fig. 6, showed that the bursts originating from the "secondary vortices" or the "transition waves" only in occasional cases were felt simultaneously and the probability for coincidence decreased drastically with increasing axial separation. As pointed out by Wei and Smith [24], the variations felt by a stationary probe might be misleading when trying to investigate structures which develop in space in a complicated way. It appears that the different phenomena related to the transition mechanisms in the shear layers and the coupling to the vortex shedding process need further elucidation.

MEASUREMENTS IN THE SUBCRITICAL REGIME

The investigation by Schiller and Linke [59] dating back to 1933 was the first to show that large changes occur in the near wake behind a circular cylinder in the Reynolds number range from about 10^3 to 10^4. They found a substantial reduction in size of the "dead air space" behind the cylinder with increasing Re in this region. This reduction was accompanied by an upstream movement of the position of laminar to turbulent transition in the shear layers. These findings were later confirmed by Bloor [23]. That the flow in this region is highly sensitive to disturbances, especially if they match the transition frequency, was demonstrated by Gerrard [10]. Also, the freestream turbulence was shown to be of great importance, see also [11]. It is therefore not surprising that the data reported in this sensitive Reynolds number range show a large scatter and it is quite clear that further measurements are needed.

Mean pressure distributions

Mean pressure distributions around the 6 mm cylinder at Re = $3 \cdot 10^3$ and $8 \cdot 10^3$ for the two turbulence intensities are shown in Fig. 9.
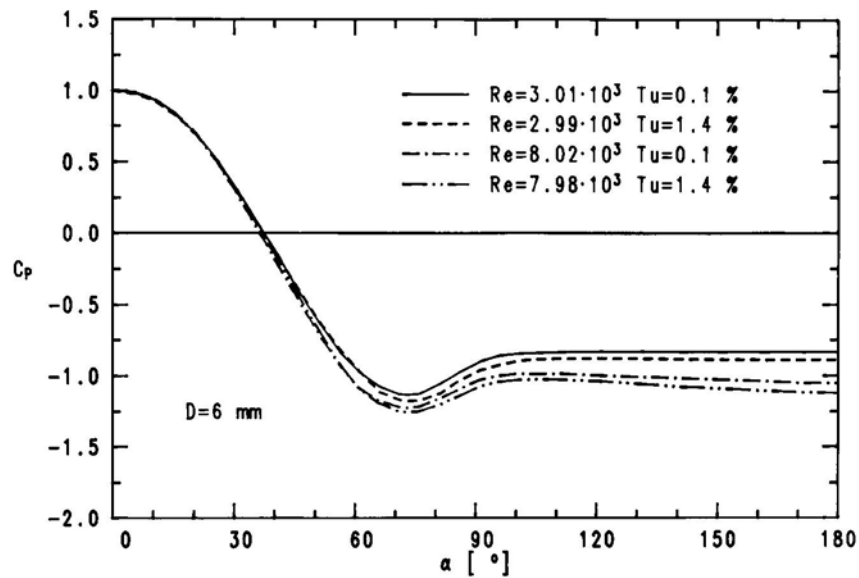

Fig. 9   Mean pressure distributions (D = 6 mm).

The cases at Re = $3 \cdot 10^3$ are both in the lower subcritical regime while the others are in the upper subcritical regime, i.e. at Reynolds numbers less than and greater than the dramatic change in the Strouhal bandwidth (see Fig. 3). The pressure distributions in Fig. 9 are not

corrected for either blockage or finite angle resolution. The effects of blockage are small for this diameter. For instance the correction method of Allen and Vincenti [60] gave a maximum correction of the freestream velocity of less than 0.3%. The corresponding maximum corrections for the mean drag coefficient (C_{Dp}) and the base pressure coefficient (C_{Pb}) were 0.6% and 1.2%, respectively. The angle occupied by the pressure tap was 7.7^o in this case and this will of course modify the pressure averaging especially in regions with strong pressure gradients. With this angular resolution the measurements by Schiller and Linke [59] indicated that the angle (α) should be reduced by about 1.6^o on the frontal part. Regarding the individual effects of Re and turbulence intensity on the C_P-distributions a division into three angular regions around the cylinder is appropriate. Up to about 30 degrees from the stagnation point ($\alpha = 30^o$) the mean pressure coefficients are more or less identical. In the region $\alpha \approx 30^o$-60° the mean pressure coefficients are lower at the higher Reynolds number the effect of the turbulence intensity being negligible. Finally, in the region between $\alpha = 60^o$ to $\alpha = 180^o$, the effects of both Reynolds number and turbulence intensity are substantial. The base pressure coefficients (C_{Pb}) at Re = 8·10^3 were about 25% lower than at Re = 3·10^3 and an increase in the turbulence intensity at the two Reynolds numbers gave a decrease in C_{Pb} of 6-7%. The decrease in the pressure coefficients implies an increase in the velocity at separation. The calculated mean pressure drag coefficients C_{Dp} and other important quantities for the cases in Fig. 9 are summarized in Table 3.

Table 3   Data for some cases with D = 6 mm.

d' – Wake width (measured at x/D=1)
L_F – Vortex formation distance
L_A – Integral axial correlation length
        (*) corrected for freestream turbulence.

Re·10^{-3}	Tu [%]	L_F/D	f_SD/U_o	C_{Dp}	-C_{Pb}	d'/D	L_A/D
3.0	0.1	2.15	0.213	0.98	0.84	1.26	10.6
3.0	1.4	1.94	0.209	1.03	0.89	1.24	9.7 (*)
8.0	0.1	1.49	0.204	1.13	1.05	1.12	5.3
8.0	1.4	1.40	0.199	1.20	1.12	1.07	4.5 (*)

Vortex formation distance and wake width

The vortex formation distance L_F was determined from the position of the maximum in the distributions of the RMS velocity along the wake centre line (y/D = 0), see Fig. 10a. As seen in Fig. 10a, the vortex formation distance decreased with increasing Re and turbulence intensity. The corresponding mean velocities measured with the hot wire (Dantec P05) along this line are shown in Fig. 10b.

(a)

(b)
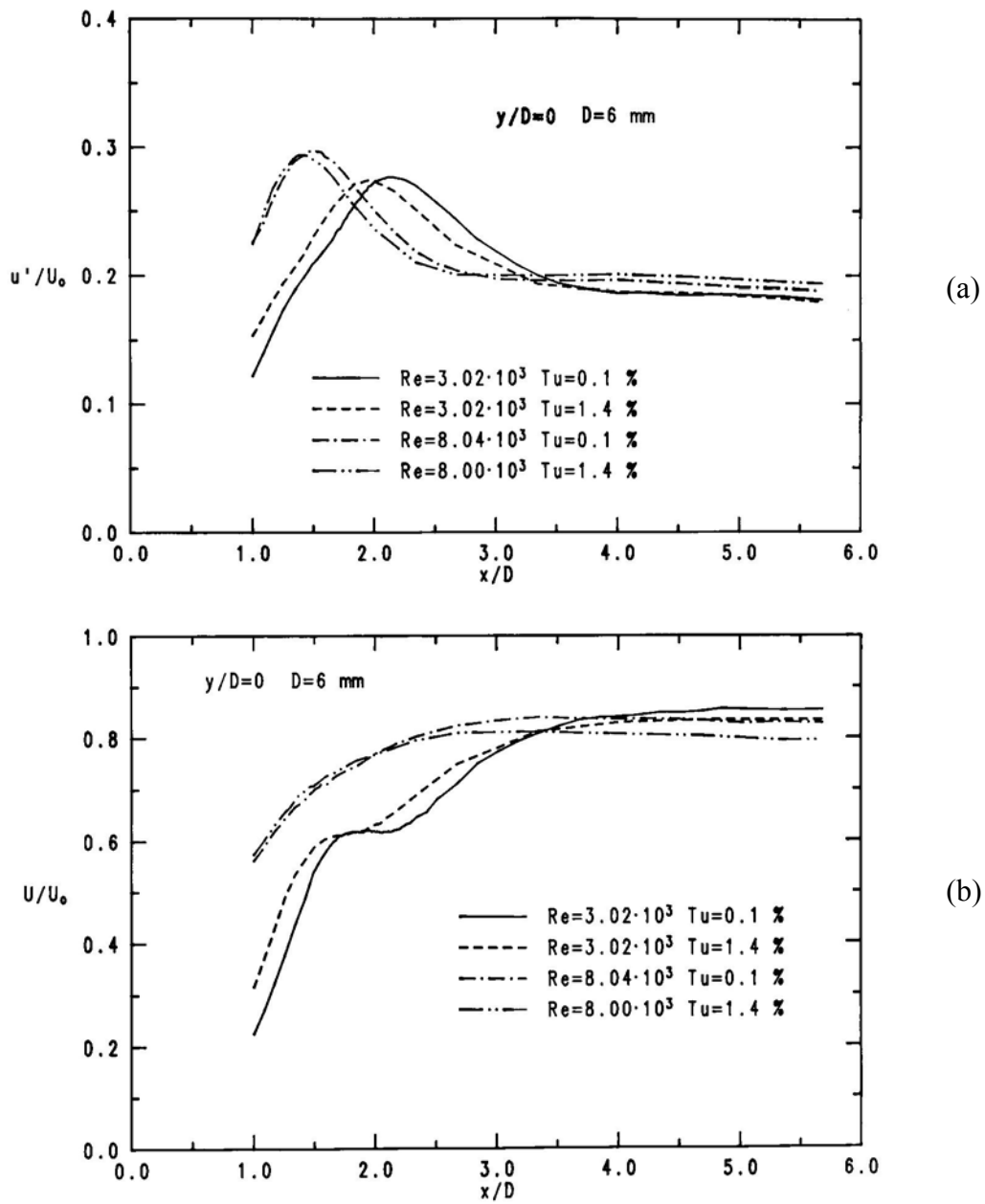
Fig. 10   Variation of (a) RMS and (b) mean velocities along wake centre line (y/D = 0).

It is noticeable that only the cases at Re = $3 \cdot 10^3$ show a plateau at a constant mean velocity in a region upstream of the position of the maximum RMS velocity. It is suspected that this behaviour is related to fundamental changes in the vortex shedding process. The so-called near-wake is generally defined as the region in which interactions between the cylinder and the separated flow occur [11]. After the vortex formation in the near-wake the vortices are convected downstream. As a consequence of the convection only minor changes of measured quantities in the streamwise direction are to be expected. The variations along the wake centre line, see Fig. 10, suggest that the near-wake region extends to about 1.5 diameters downstream of the vortex formation point (x = L_F).

The variation of the RMS velocity and of the flatness factor of the velocity fluctuations along the line x/D = 1 are shown in Fig. 11.
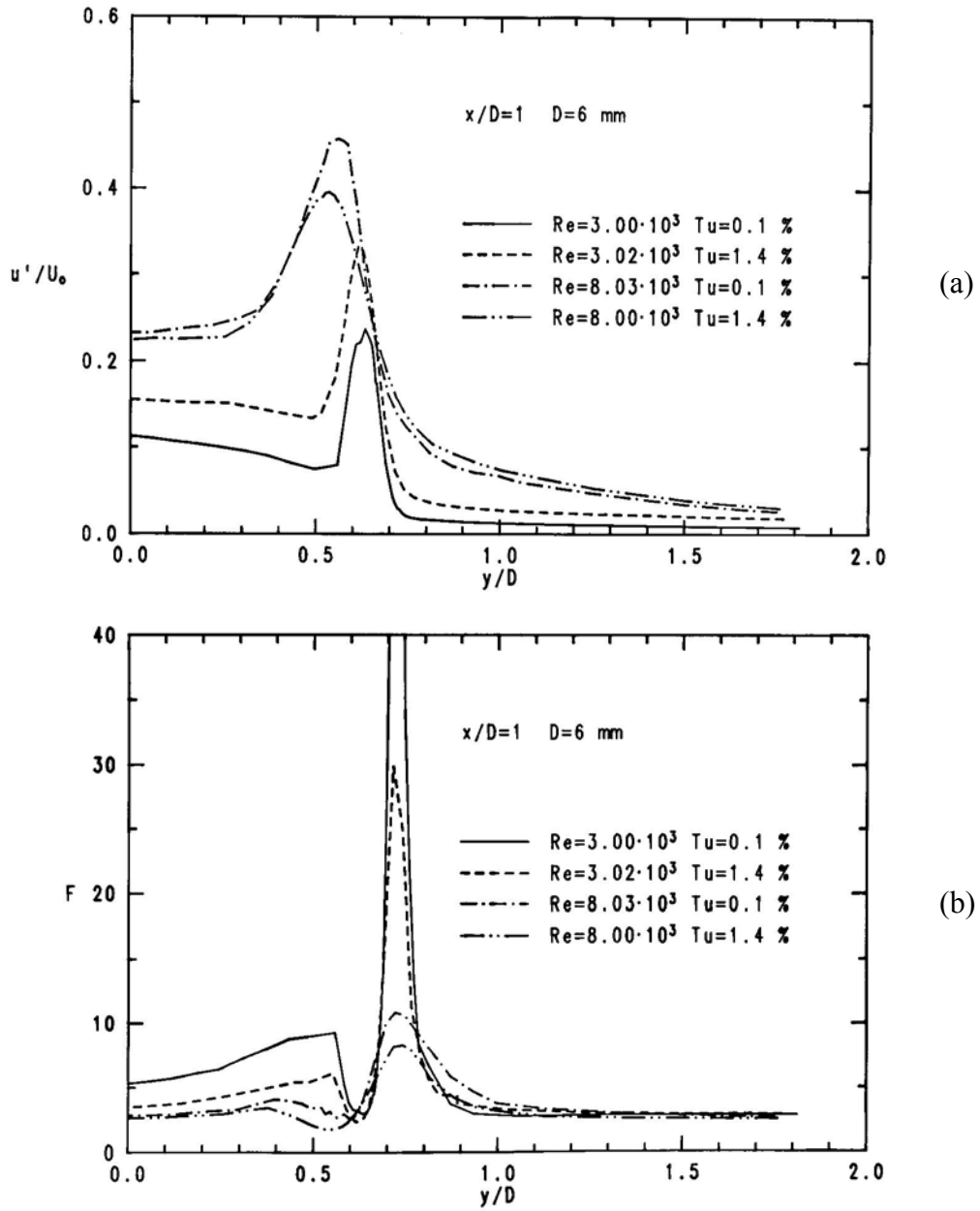
Fig. 11   Variation of (a) RMS (u') and (b) flatness factor (F) of velocity fluctuations at x/D = 1.

A slight difference between the two sides of the wake was anticipated from the asymmetry enforced by the probe support. However, only minor changes in the levels were noticed and the positions of extreme values were perfectly symmetric with respect to the oncoming flow direction. It should be pointed out that the absolute values, especially in the recirculating regions, should be treated with caution. The distance between the positions of the maximum in the RMS distributions at x/D = 1 was used as an estimate for the wake width (d') at this

location. This wake width appears to have a similarity with the wake width as determined from Roshko's "notched hodograph theory" [61]. The decrease in d'/D with increasing Re and Tu is related to the decrease in the vortex formation length. Boundary layer calculations using the experimental pressure distributions in Fig. 9 indicated that the separation occurred at $\alpha \approx 80^o$. It was noticed that the increase in Re and Tu gave a slight reduction in the separation angle. As seen in Table 2 the Strouhal number decreased slightly with decreasing vortex formation length. The reduction in L_F/D (and d'/D) together with an increase in the velocity at separation imply an increase in the Strouhal number [62]. Gerrard [47] introduced the so-called diffusion length in order to explain the observed Strouhal number variation. He argued that the diffusion length, which is a measure of the width of the separated shear layers, is expected to increase with decreasing L_F/D and thus a balance between these scales explains the relative constancy of the Strouhal numbers. The intermittent nature of the velocity fluctuations in the outer parts of the shear layers is reflected in the high values of the flatness factor in these regions. The position of the maximum of this factor can be used as an estimate for the outer limit of the shear layer [31]. As seen in Fig. 11b, this position was more or less the same for the different cases (y/D ≈ 0.72). In [31] the difference between the positions of maximum flatness factor and maximum RMS-velocity at constant x/D was used as a measure for the width of the shear layer. As seen in Fig. 11, this width increases with decreasing L_F/D. In Fig. 12 some earlier measurements of the vortex formation distance are collected together with the present data.
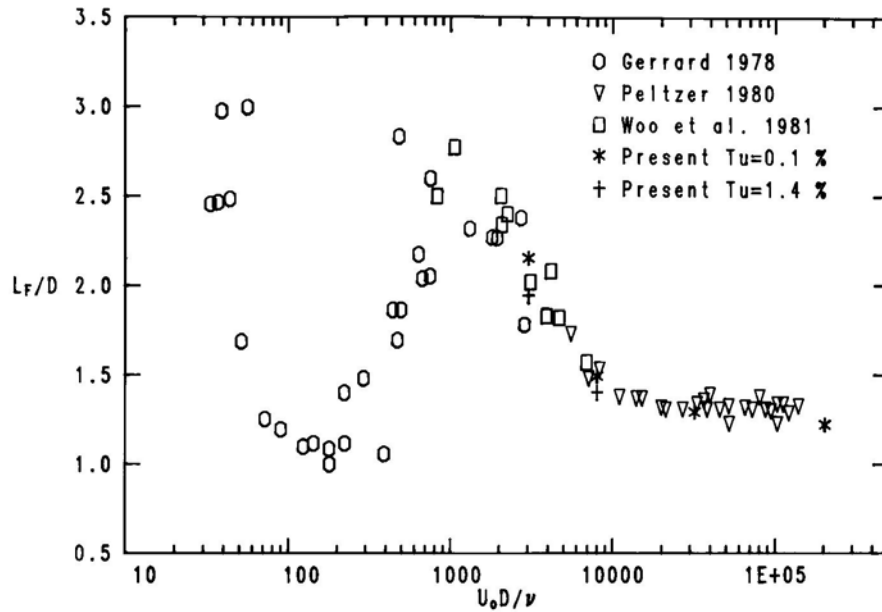

Fig. 12   Vortex formation length vs Reynolds number.

The vortex formation lengths in Fig. 12 from the paper by Gerrard [13] were determined from the points closest to the cylinder at which irrotational fluid crosses the wake centre line (flow visualization). It has been shown by Bloor and Gerrard [63] that this definition is compatible with the definition used in this paper (same as in [30, 64, 65]). The data of Gerrard, see Fig. 12, suggest that the vortex formation length has a minimum in the transition regime. The formation lengths of Bloor [23] and Schiller and Linke [59] are in general agreement with the data compiled in Fig. 12. It appears that the formation length has a maximum of about 3 diameters at a Reynolds number slightly above 10^3. It then decreases rather rapidly up to about $Re = 10^4$. The effect of the higher turbulence intensity is to accelerate this process. The vortex formation length levels out at a value of about 1.2 diameters in the upper end of the subcritical regime. Gerrard [47] has shown that the shrinking of the formation region is related to the upstream movement of the position of transition in the shear layers. The vortex formation length is also closely related to the base pressure coefficient C_{Pb}; a decrease in L_F increases the curvature of the streamlines associated with vortex formation thus producing a decrease of the base pressure. As seen in Table 2 the relative changes of these quantities are of the same magnitude, see also Figs. 12 and 15.

Some rationale for the sub-division of the subcritical regime at about $Re = 5 \cdot 10^3$ can be found from the dramatic changes in the RMS lift coefficient and in the Strouhal bandwidth at around this Reynolds number, see e.g. [33] and Fig. 3. Gerrard [47] noted that the decrease in L_F/D could only explain a part of the observed changes in the RMS lift coefficient. This lead him to suggest a possible fundamental change in the mode of vortex formation. He speculated on the possibility that the vortex sheets might develop independently of each other at Reynolds numbers below the transition. In that case the fluctuating lift on the cylinder should attain small values because the transverse momentum flux may be balanced by fluid motions rather than from body forces [13]. Blevins [25] found that the vortex shedding in the upper subcritical regime seems to consist of strings of coherent cyclic events, which have frequencies that wander about the mean vortex shedding frequency. This explains the increased Strouhal bandwidth at these Reynolds numbers. Another important feature in the upper subcritical regime is the large amplitude modulations of the signals associated with vortex shedding. It has been suggested, see e.g. [66], that the pulsations are due to slow variations in the size of the formation region. The soundness of this explanation can be found from the fact that the frequency associated with large amplitudes seems to be lower than in the intervals with lower amplitudes, see e.g. [25, 34].

<u>Axial correlations</u>

The measurements by Leehey and Hanson [67] indicated that the axial correlation decreases significantly at Reynolds numbers from about $3 \cdot 10^3$ to 10^4. Prendergast [68] and el-Baroudi [69] have presented axial correlations in the Reynolds number range 10^4 to 10^5, which showed that the axial correlation increases slightly up to about Re = $5 \cdot 10^4$ and then decreases when approaching the critical regime at higher Re. It was decided to further investigate the axial correlations and to see whether any fundamental changes occur when going from the lower to the upper subcritical regime. The correlation measurements were carried out using two hot wires (Dantec P15) at various separations in the axial direction. The signals were band-pass filtered with a low cut-off frequency of 1 Hz and a high cut-off frequency approximately equal to $2.5 \cdot U_o/D$. One hot wire was held stationary while the other was movable in all directions. With the 6 mm cylinder the hot wires were positioned at x/D = 0.4, y/D = 0.9 and at x/D = 0.0, y/D = 0.57 with the 41 mm cylinder. At these positions, outside the shear layers, the velocity fluctuations contain a component that is directly related to the freestream turbulence (RMS velocity = t'). If one assumes that the fluctuating velocity due to the freestream turbulence is uncorrelated with the remaining velocity fluctuations (RMS velocity = v') then the measured cross-correlation coefficient ρ_{12} between the two stations can be written as:

$$\rho_{12} = (\rho_{12}^{v} + r^{-2}\rho_{12}^{t})/(1 + r^{-2})$$

where ρ_{12}^{t} and ρ_{12}^{v} are the cross-correlation coefficients between the two stations due to the freestream turbulence and due to the remaining flow components, respectively; r is the signal-to-noise ratio defined as the ratio between the RMS values for the two components (r = v'/t', $(u')^2 = (v')^2 + (t')^2$, u' = RMS velocity at the hot wire position). It is evident from the expression above that it is desirable to have a large signal-to-noise ratio in order to reduce the influence from the freestream turbulence. In the real situation a coupling between the components is likely but it is reasonable to assume that this coupling is small for the cases investigated (i.e. at the present relative positions of the hot wires). For the cases with Tu = 0.1% the effects from the freestream turbulence on the measured correlation coefficients were considered negligible (r >10). Uncorrected axial correlation coefficients at three Reynolds

numbers (Tu = 0.1%) are shown in Fig. 13a. For the cases at Tu = 1.4% (see Table 2) the signal-to-noise ratios were about 1 at Re = $3 \cdot 10^3$ and about 2 at Re = $8 \cdot 10^3$. The corrected correlation coefficients (ρ_{12}^{v}) for these cases are shown in Fig. 13b.
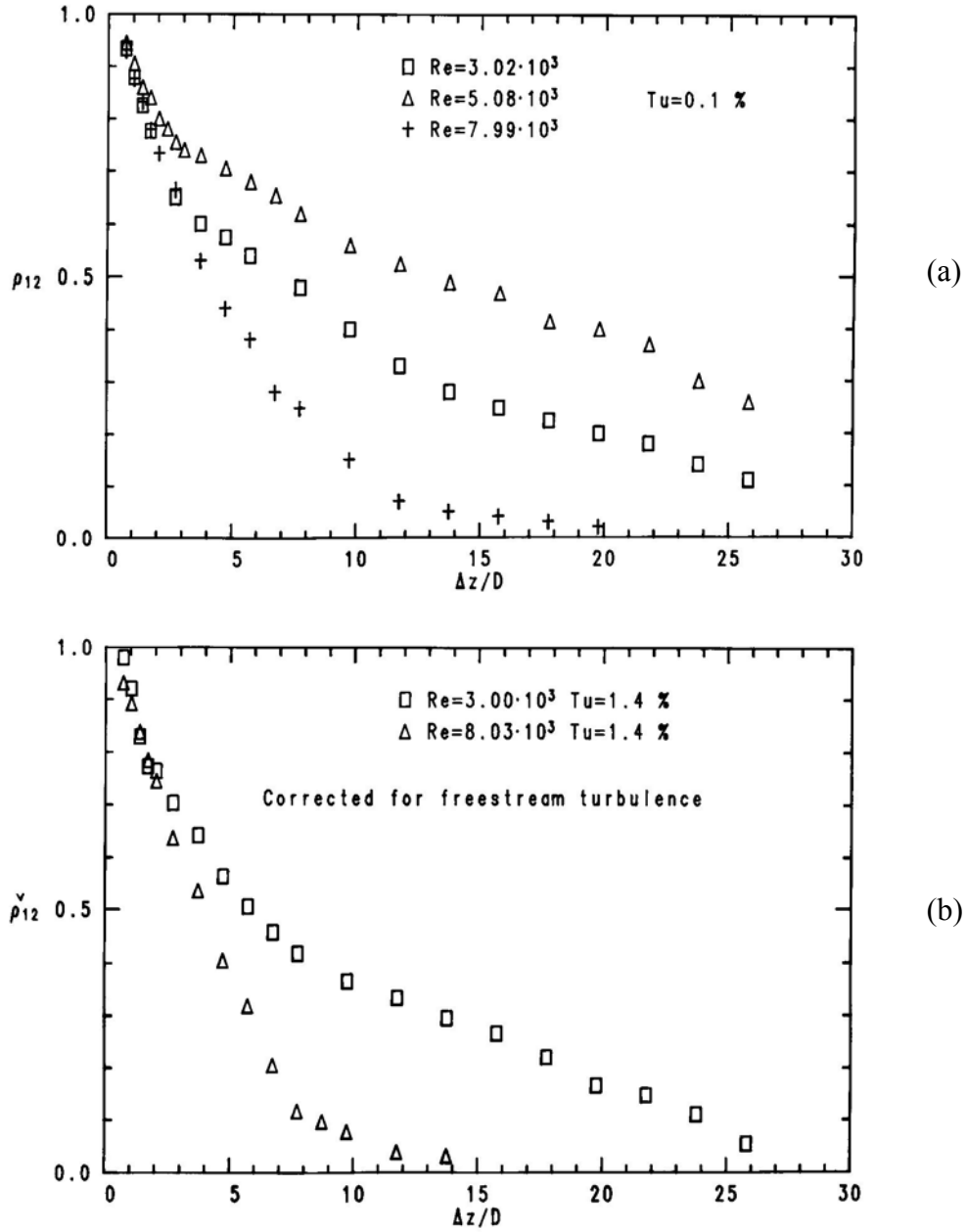
Fig. 13 Cross-correlation coefficients in the axial direction. (a) Uncorrected Tu = 0.1%, (b) Corrected for freestream turbulence (see text) Tu = 1.4%.

The correlation coefficient ρ_{12}^t was estimated using the longitudinal integral length scale Λ ($\Lambda/D = 2$, see Table 1) [70]:

$$\rho_{12}^t \approx (1 - \Delta z / 2\Lambda)\,e^{-\Delta z / \Lambda}$$

The integral axial correlation lengths L_A (one-sided) were calculated for the different cases in Fig. 13. In the cases with finite correlation at the maximum separation distance ($\Delta z/D = 26$) the data had to be extrapolated in order to obtain the integral axial correlation length. For the case at $Re = 5 \cdot 10^3$, $Tu = 0.1\%$ (not included in Table 3) a noticeable high degree of phase uniformity along the axis was found ($L_A/D = 16.2$).

It is also noticeable that the correlation coefficients for the upper subcritical cases at $Re = 8 \cdot 10^3$ show a decrease at large separations which is completely different from the others. The variation of the cross-correlation coefficient at the axial separations $\Delta z/D = 2.2$ and 6.0 with Reynolds number at $Tu = 0.1\%$ is shown in Fig. 14.
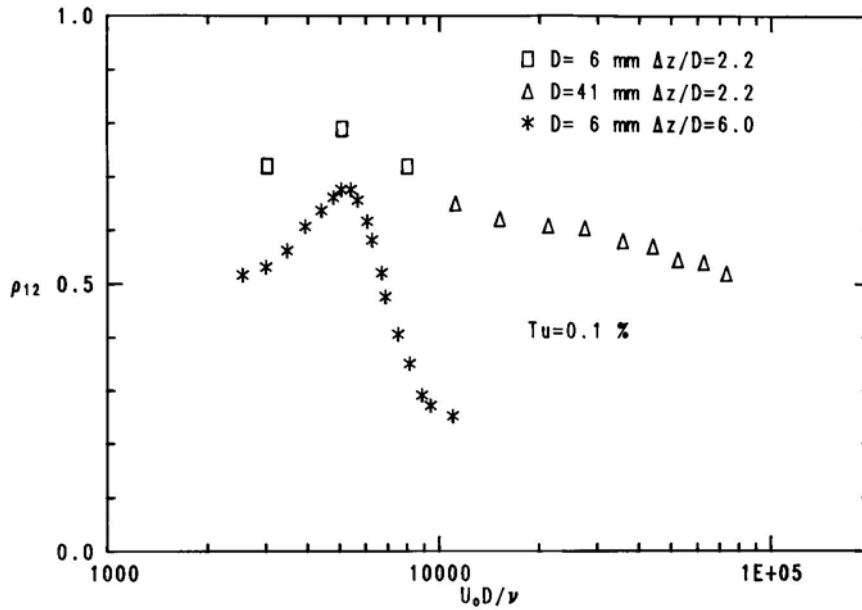
Fig. 14 Cross-correlation coefficient at axial separations of 2.2 and 6 diameters vs Reynolds number, Tu = 0.1%.

It is evident from Fig. 14 that a maximum correlation occurs at a Reynolds number just above $5 \cdot 10^3$. This Reynolds number coincides with the Reynolds number where the Strouhal bandwidth changes dramatically, see Fig. 3. Thus it seems likely that a fundamental change in the vortex shedding process occur at around $Re = 5 \cdot 10^3$ ($Tu = 0.1\%$). The variations of the

correlations at fixed axial separations with additional freestream turbulence (Tu = 1.4%) were not explored in detail. It is reasonable to believe that similar variations as those shown in Fig. 14 occur at the higher turbulence intensity. The only fundamental differences are expected to be a shift to lower Reynolds numbers and a lowering of the maximum value. The nature of the flow mechanism responsible for the seemingly fundamental changes at Re $\approx$ $5 \cdot 10^3$ (Tu = 0.1%) and Re $\approx 4 \cdot 10^3$ (Tu =1.4%) is not fully understood at the present time. It looks as if the vortex shedding changes from one mode that is correlated over very large axial distances with a well-defined frequency to a mode in which the shedding frequency changes with time the axial correlations being much smaller. A deeper understanding of the change in the vortex shedding mode cannot be expected until the time we know much more about the three-dimensional features in the flow mechanisms at both high and low Reynolds numbers in the subcritical regime.

The measurements by Leehey and Hanson [67] indicated a steady decrease in the axial correlation length in the Reynolds number range around $5 \cdot 10^3$. In their case the cylinder was forced to vibrate but the amplitude of the cylinder vibration was less than 3% of the diameter in the worst case (at third harmonic resonance). It was believed that the cylinder vibration was insufficient to cause any increase in the correlation length. The present correlation lengths at Tu = 1.4% (corrected) are in reasonable agreement with the data of Leehey and Hanson although they reported a turbulence intensity of about 0.04%. The large discrepancy between the present data at Tu = 0.1% and the data of Leehey and Hanson especially concerning the presence of a maximum correlation at around Re = $5 \cdot 10^3$ is intriguing. In the mounting arrangement of Leehey and Hanson the cylinder was exposed to uniform flow except within the shear layers of the open-jet. They reported that the thickness of the shear layer was about 8 cylinder diameters. The length exposed to uniform flow was however about 80 diameters but the effect of end conditions might still be crucial especially regarding the three-dimensional aspects of the flow. It is worth noting that Leehey and Hanson measured a negative correlation at large axial separations (Re = $6.05 \cdot 10^3$). This seemingly erroneous behaviour was not observed in the present measurements. Nevertheless, the same principal variations regarding the decay of the axial correlations at different Reynolds numbers is evident from the additional data of Leehey and Hanson as given in [33].

The variation of the cross-correlation coefficient for $\Delta z/D = 2.2$, see Fig. 14, indicates that the axial correlation length is relatively constant (slowly decreasing) at Reynolds numbers between say 10^4 and 10^5. The measurements by Prendergast [68] (correlations between the

wall pressures at the shoulder of the cylinder) indicated an increase in L_A/D from about 3 at $Re = 3 \cdot 10^4$ to about 4 at $Re = 9 \cdot 10^4$. El-Baroudi [69] found from velocity correlations at the shoulder an increase in L_A/D from about 3 at $Re = 10^4$ to about 6 at $5 \cdot 10^4$. A decrease in the correlation length with increasing Re in the upper subcritical regime has been reported by Kacker et al. [71], Bruun and Davies [72] and Sonneville [49]. Thus it appears that more measurements on the axial correlations are needed in the subcritical regime. One problem in the conventional way of measuring a cross-correlation is the effects due to extraneous noise. In some cases the cross-correlations can be corrected afterwards (see above) and in some cases a suitable filtering might solve the problem. In any case it must be specified which components in the flow the cross-correlation should be based on. If it is possible to sort out the components in the frequency domain the use of coherence functions [25] or band-pass filters might be effective.

BASE PRESSURE COEFFICIENTS

Mean base pressure coefficient

Roshko and Fiszdon [11] presented an overall view on various transition phenomena that occur in the flow around a circular cylinder. The basis of their discussion was the existing data (up to 1969) on the variation of the Strouhal number and of the (mean) base pressure coefficient. In particular, a comparison between their own data and data of Gerrard [10] on C_{Pb} in the Re range from 10^3 to 10^5 was presented. The comparison clearly demonstrated the sensitivity to the freestream turbulence intensity but there was also a noticeable effect of the cylinder diameter. As plausible reasons for the diameter effect they mentioned the scale of turbulence and effects of the wall constraints. In 1982, West and Apelt [73] presented data on the separate effects of blockage and aspect ratio in the Re range from 10^4 to 10^5. They found that a reduction in the aspect ratio (end plates were used) gave similar effects on e.g. C_{Pb} as an increase in the blockage. The effects of the aspect ratio seemed to be more prominent at the lower end of the Re range considered (i.e. near $Re = 10^4$). This is consistent with the decreasing axial correlations with Re found in this investigation, see Fig. 14. The present results on the base pressure coefficient can be found in Fig. 15.
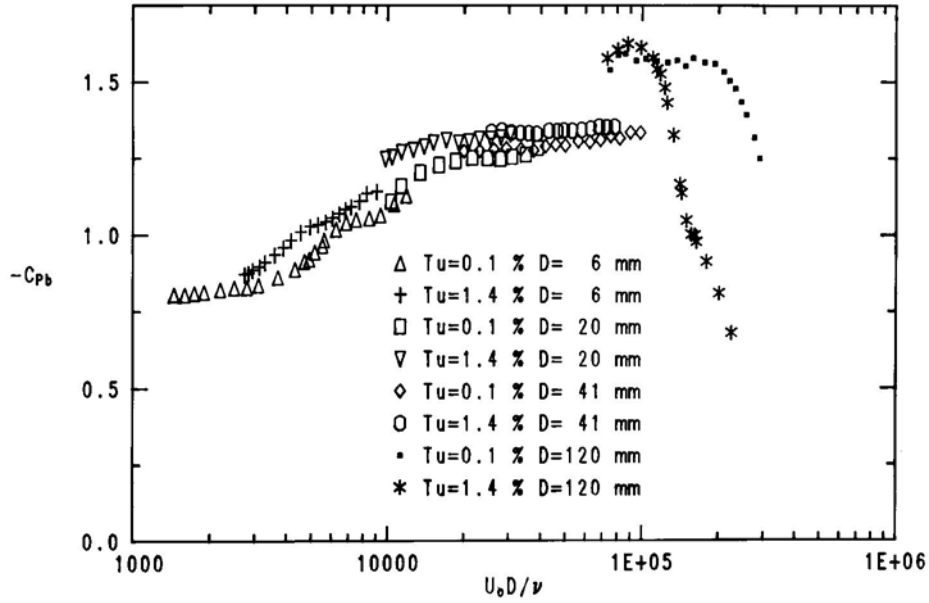
Fig. 15   Mean base pressure coefficient vs Reynolds number for Tu = 0.1% and 1.4%.

The results for the 41 mm and 120 mm cylinders have been reproduced from an earlier paper [30]. In the intervals with overlapping the effects from the diameters can be judged. It is worth noting; see also [30], that the effects of the freestream turbulence, in the overlapping regions, were more or less independent of the diameter. Conventional corrections for the blockage effect; see e.g. [73], are questionable in regions where the actual shape of the pressure distributions changes with Reynolds number (and blockage). It was however noticed that an excellent continuity in the variation with Re could be reproduced when applying constant correction factors for the different diameters. The optimum correction factors for the freestream velocity (U_o) and for C_{Pb} were found to be: 1.003, 0.99 (D = 6 mm); 1.005, 0.98 (D = 20 mm); 1.01, 0.96 (D = 41 mm) and 1.06, 0.81 (D = 120 mm), respectively. The present corrected and somewhat smoothed data are depicted in Fig. 16. Smoothed data from Thom [74, 75] and Gerrard [10] at low Reynolds numbers and data points from Bearman [48] are also included in Fig. 16. Please note that the negative of C_{Pb} is shown in Figs. 15 and 16.

38
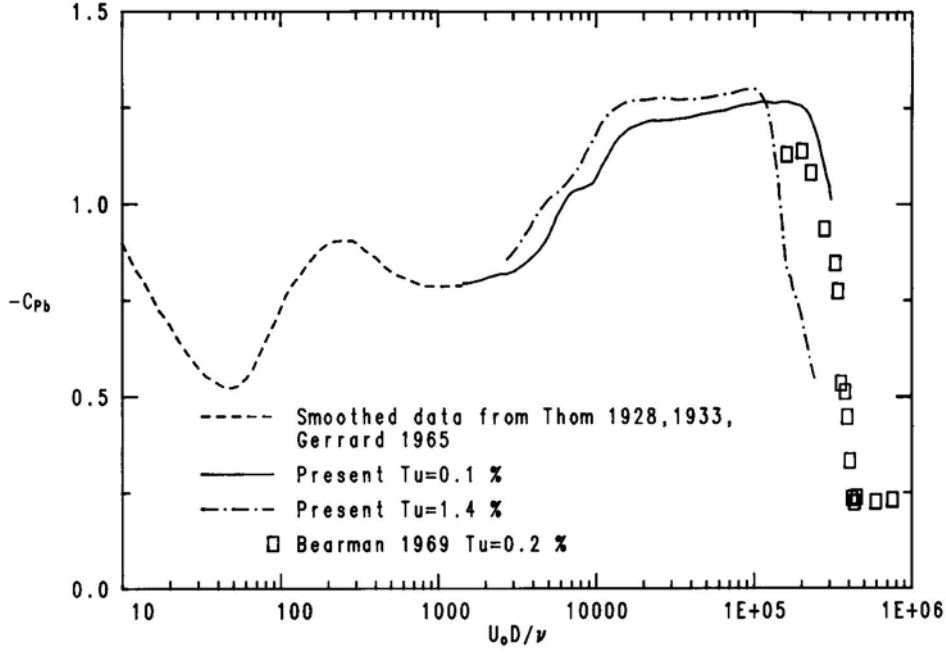
Fig. 16 Variation of the mean base pressure coefficient in the Reynolds number range from 10 to 10^6.

One interesting point is that C_{Pb} for Tu = 1.4% reaches a lower level than for Tu = 0.1% before the increase when entering the critical regime. The C_{Pb}-variation at the two turbulence intensifies could be made more or less identical up to about Re = 10^5 by multiplying the Reynolds numbers at Tu = 1.4% with a factor of about 1.25 when at the same time adding 0.03 to the levels in C_{Pb}. Keeping the same addition to the levels (ΔC_{Pb} = 0.03) but now multiplying the Reynolds numbers at Tu = 1.4% with a factor of about 2 gave coincidence in the variations from about Re = $3 \cdot 10^4$ to Re = $3 \cdot 10^5$. Thus it can be concluded that a constant factor multiplying Re, in the sense of an effective Reynolds number, was not applicable to the present data. It should be remembered that the scale of the turbulence was approximately constant, i.e. the relative scale decreases with increasing diameter, see Table 1. It appears from available data, see e.g. [76], that small-scale turbulence is more effective in accelerating the transition processes that occur when entering the critical regime. A high sensitivity to disturbances having a frequency in coincidence with the transition frequency (f_T) has previously been observed, see e.g. [10]. The scale of the "secondary vortices" associated with the transition in the shear layers can be estimated as the ratio between their convection velocity to the transition frequency. As shown by e.g. Yamanaka et al. [55] the convection velocity for the "secondary vortices" is of the same order as the convection velocity for the vortex street, which in turn is slightly lower than the freestream velocity. The fact that f_T/f_S increases with Re at a relatively constant Strouhal number implies that the most susceptible

39

scale of turbulence decreases with Re. For instance the value of $f_T/f_S \approx 40$ at Re $= 10^5$, see Fig.8, would give a most susceptible scale of about 0.1 diameters. This is about the same relative scale as for the 120 mm cylinder; see Table 1. Also interactions with other scales in the flow, for instance relevant scales in the near wake and scales in the spanwise direction, might be important in the transition mechanisms involved.

The smoothed variation of C_{Pb} at Reynolds numbers less than about 10^3, see Fig. 16, is rather tentative due to the large scatter of the data reported in this region. Nevertheless, the extreme values seem to be in coincidence with major transitions in the flow. For instance the base pressure coefficient appears to have a local maximum at around the onset of vortex shedding at Re ≈ 50 and a local minimum in the transition regime. The reader is referred to the papers by Roshko and Fiszdon [11] and Gerrard [13] for a more complete discussion about the variations at these Reynolds numbers.

The variation of C_{Pb} at Re greater than about 10^3 generally follows the variation of the vortex formation length; see Fig. 12. It appears however that the rate of change in C_{Pb} is slowed down at around a Reynolds number slightly above the limit between the lower and upper subcritical regime. The observed C_{Pb}-variation might be a reflection of that the axial correlation as well as the vortex formation length changes substantially in this Reynolds number range. The change to a slow variation of C_{Pb} with increasing Re occurs at about Re $= 10^4$. At this stage the transition point in the shear layer has reached a position quite close to the cylinder [23]. The upstream movement of the transition continues with increasing Re but at a decreased rate; the transition has almost reached the separation point at the upper end of the subcritical regime.

In the so-called precritical regime [28] the separation moves downstream with increasing Re and as a consequence the base pressure coefficient increases, the wake becomes narrower and the Strouhal number increases. In the so-called paracritical regime [28] the laminar separation is followed by a separation bubble, reattachment and subsequent turbulent separation. Evidence of that the separation bubble only forms at one side which results in a steady lift force on the cylinder have been reported in a number of investigations, see e.g. [48, 77, 78]. As demonstrated by Schewe [79] the asymmetric behaviour is very sensitive to disturbances in the flow. Schewe interpreted the symmetry breaks with jumps to different critical flow states with associated hysteresis effects as so-called subcritical bifurcations [78]. As noted in [30] the present case at Tu $= 1.4\%$ did not appear to have similar breaks in the symmetry. This was believed to be a result of a smearing effect due to the small-scale turbulence. In other

words the equilibrium flow states and how they change with changes in the leading parameter, i.e. the Reynolds number, may be completely different when considering cases with different flow conditions (e.g. freestream turbulence, surface roughness, ...). It is worth noting that both the present C_{Pb}- and Strouhal number variations at Tu = 0.1%, Re < $3 \cdot 10^5$ compare favourable with the results of Bearman [48], see Figs. 4b and 16. Bearman did observe asymmetric flow in the critical regime at Re > $3 \cdot 10^5$ but limitations in the tunnel speed did not permit measurements at such high Reynolds numbers in the present case (D = 120 mm).

RMS base pressure coefficient

The RMS pressure coefficient C_P' is defined as the ratio between the RMS value of the wall pressure fluctuations to the dynamic pressure. The variation of C_P' around the cylinder for some cases with the 41 mm and 120 mm cylinders in the subcritical regime (Tu = 0.1%, 1.4%) and in the critical regime (Tu = 1.4%) can be found in [30]. The variation of the RMS pressure coefficient at α = 180° (C_{Pb}') with Reynolds number at the two turbulence intensities are shown in Fig. 17. Corrections for blockage have been applied to the freestream velocities (same corrections as in Fig. 16) but not to the C_{Pb}'-values. The expected increase in C_{Pb}' due to an increase in blockage is evident in the overlapping regions of the 20 mm and 41 mm cylinders but not in the corresponding joints between the 41 mm and 120 mm cylinders. As shown in an earlier paper [31] about 35 % of the fluctuation energy in the base region comes from frequencies less than $0.1 \cdot U_o/D$. At Re ≈ 10^5 the value of $0.1 \cdot U_o/D$ is about 11 Hz for the 120 mm cylinder. The low-frequency limit of the microphones used (B & K type 4135) was about 3 Hz (-3 dB). Thus it can be inferred that the C_{Pb}'- values measured with the 120 mm cylinder are to low in the lower end of the Reynolds number range with this diameter. Without taking this effect in consideration the maximum relative error in these measurements was estimated to be less than 3% [30].
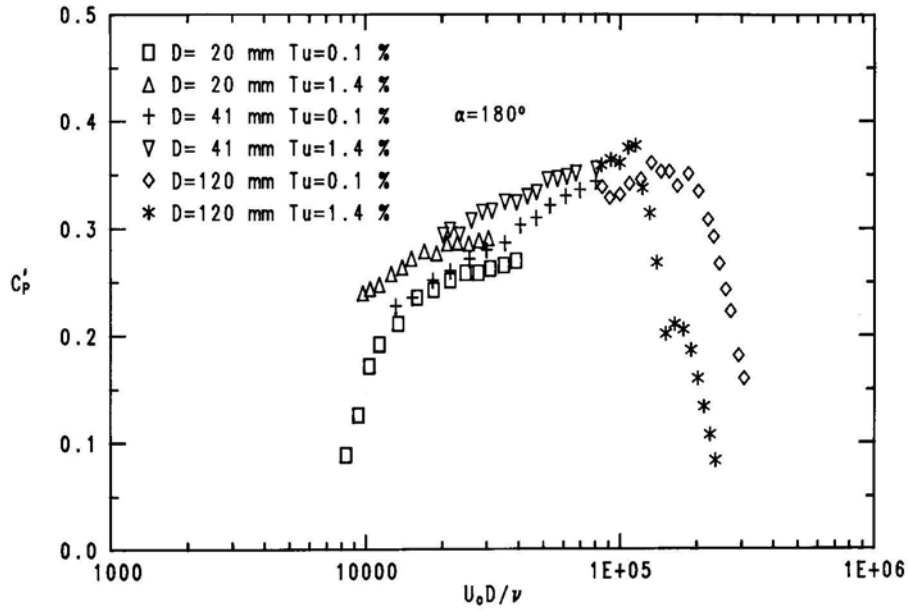
Fig. 17   RMS base pressure coefficient vs Reynolds number for Tu = 0.1% and 1.4%.

As seen in Fig. 17, the RMS base pressure coefficient increases dramatically with increasing Re at Re $\approx 8 \cdot 10^3$ (Tu = 0.1%). This is presumably connected to the transition at about Re = $5 \cdot 10^3$ at this turbulence intensity. It is worth noting the seemingly clear connection between the RMS base pressure coefficient, the turbulence intensity at the shoulder of the cylinder, see e.g [10, 30], and the sectional RMS lift coefficient [30]. The RMS base pressure coefficients at the two turbulence intensifies show a rather steady increase from about Re = 10^4 to the sudden decrease when entering the critical regime. A comparison with the variations in the mean pressure coefficient shows that a decrease in C_{Pb} is connected to an increase in C_{Pb}' This coupling between the coefficients is a reflection of that both the mean velocities and the velocity fluctuations in the base region increase as a consequence of the shrinking of the formation region.

CONCLUSIONS

The present paper provides additional experimental information on the flow around a circular cylinder in cross flow. By using cylinders with various diameters in a wind tunnel, the Reynolds number (Re) was varied from about 50 to $2 \cdot 10^5$. Results were presented for two turbulence intensities in the oncoming flow (Tu = 0.1% and 1.4%). Within the experimental accuracy, the Strouhal numbers were unaffected by the freestream turbulence for Reynolds numbers less than about 10^3. At these Re, the integral length scale of the freestream

turbulence was relatively large compared to the cylinder diameters. The results on the corresponding bandwidths of the shedding frequency (Δf_S) suggest that the shedding frequency (f_S) responds instantaneously to the velocity variations imposed by the freestream turbulence ("quasi-stationary flow").

Regardless of the turbulence intensity, the Reynolds number at which the vortex shedding started was about 48, the onset value of the Strouhal number being 0.117. The present Strouhal numbers were found to vary continuously with Re in the stable regime. The results indicated that the transition regime extended from Re $\approx$ 160 to Re $\approx$ 265. The relative bandwidth ($\Delta f_S/f_S$) increased up to a maximum of about 5% in the transition regime.

The present Strouhal number data were compared with some existing proposals for the Strouhal - Reynolds number relationship. The present data was found to be a support for the so-called "Roshko relation" in the stable regime.

In the Reynolds number range from about $2 \cdot 10^3$ to $5 \cdot 10^4$ (Tu = 0.1%) some data on the ratio between the shear layer transition frequency to the shedding frequency were given. The present data indicated that the increase of the ratio with Re was greatest at Re $\sim 5 \cdot 10^3$.

At Reynolds numbers greater than about 10^3 the flow was dependent on the turbulence intensity. For instance, the Strouhal numbers were lower at the higher turbulence intensity in the Re-range from about 10^3 to 10^5 the difference being greatest around Re = $5 \cdot 10^3$.

The flow seemed to exhibit a basic change at a Reynolds number of about $5 \cdot 10^3$ ($4 \cdot 10^3$ with turbulence). A sub-division of the subcritical regime at this Reynolds number is proposed. At the boundary between the so-called lower and upper subcritical regimes the relative bandwidth changed by about one order of magnitude. In addition, the axial correlations appeared to have a local maximum at this Re. Probably, the vortex shedding changes from one mode that is correlated over large axial (spanwise) distances with a well-defined frequency to a mode in which the shedding frequency varies with time, the axial correlations being much smaller. Further measurements are needed in order to clarify the apparent change in the mode of vortex shedding.

In the beginning of the upper subcritical regime the axial correlations showed a rapid decrease with increasing Re. Also the mean and RMS base pressure coefficients changes dramatically in this region. In the Reynolds number range from about 10^4 to the end of the subcritical regime at around $2 \cdot 10^5$ ($1 \cdot 10^5$ with turbulence) both the mean and RMS base pressure

coefficients show a rather slow variation with Re; the coefficients (absolute values) at Tu = 1.4% being greater than those at Tu = 0.1%.

ACKNOWLEDGEMENTS

REFERENCES

1   Strouhal, V., Ueber eine besondere Art der Tonerregung, Ann. Phys. und Chemie, Neue Folge, Vol. 5, No. 10, pp. 216-251 (1878)

2   Richardson, E. G., Aeolian tones, Proc. Phys. Soc. London, Vol. 36, pp. 153-167 (1924)

3   Bénard, H., Formation de centres de giration à l'arrière d'un obstacle en mouvement, Acad. Sci. Comptes Rendus (Paris), Vol. 17, pp. 839-842 (1908)

4   von Kármán, T. and Rubach, H., Über den Mechanismus des Flüssigkeits- und Luftwiderstandes, Phys. Zeitschrift, Vol. 13, No. 2, pp. 49-59 (1912)

5   Bénard, H., Sur les écarts des valeurs de la fréquence des tourbillons alternés par rapport à la loi de similitude dynamique, Acad. Sci. Comptes Rendus (Paris), Vol. 183, pp. 20-22 (1926)

6   Lord Rayleigh, Aeolian tones, Phil. Mag. Ser. 6, Vol. 29, pp. 433-444 (1915)

7   Gerich, D. and Eckelmann, H., Influence of end plates and free ends on the shedding frequency of circular cylinders, J. Fluid Mech., Vol. 122, pp. 109-121 (1982)

8   Stansby, P. K., The effects of end plates on the base pressure coefficient of a circular cylinder, Aeronautical Journal, Vol. 78, pp. 36-37 (1974)

9   Fage, A. and Warsap, J. H., The effects of turbulence and surface roughness on the drag of a circular cylinder, ARC Reports and Memoranda No. 1283 (1929)

10   Gerrard, J. H., A disturbance-sensitive Reynolds number range of the flow past a circular cylinder, J. Fluid Mech., Vol. 22, Part 1, pp. 187-196 (1965)

11   Roshko, A. and Fiszdon, W., On the persistence of transition in the near-wake, in Problems of Hydrodynamics and Continuum Mechanics, Philadelphia, pp. 606-616 (1969)

12   Homann, F., Einfluβ groβer Zähigkeit bei Strömung um Zylinder, Forsch. Ing. -Wes., Vol. 7, No. 1, pp. 1-10 (1936)

13   Gerrard, J. H., The wakes of cylindrical bluff bodies at low Reynolds number, Phil. Trans. Roy. Soc. (London) Ser. A, Vol. 288, No. 1354, pp. 351-382 (1978)

14   Coutanceau, M. and Bouard, R., Experimental determination of the viscous flow in the wake of a circular cylinder in uniform translation. Part 1. Steady flow, J. Fluid Mech., Vol. 79, Part 2, pp. 231-256 (1977)

15   Kovásznay, L. S. G., Hot-wire investigation of the wake behind cylinders at low Reynolds numbers, Proc. Roy. Soc. (London) Ser. A, Vol. 198, pp. 174-190 (1949)

16   Roshko, A., On the development of turbulent wakes from vortex streets, NACA Report 1191 (1954)

17   Schaefer, J. W. and Eskinazi, S., An analysis of the vortex street generated in a viscous fluid, J. Fluid Mech., Vol. 6, pp. 241-260 (1959)

18   Tritton, D. J., Experiments on the flow past a circular cylinder at low Reynolds numbers, J. Fluid Mech., Vol. 6, Part 4, pp. 547-567 (1959)

19   Berger, E., Die Bestimmung der hydrodynamischen Gröβen einer Kármánschen Wirbelstraβe aus Hitzdrahtmessungen bei kleinen Reynoldsschen Zahlen, Zeitschrift Flugwiss., Vol. 12, No. 2, pp. 41-59 (1964)

20   Sreenivasan, K. R., Transition and turbulence in fluid flows and low-dimensional chaos, in Frontiers in Fluid Mechanics, Springer-Verlag, pp. 41-67 (1985)

21   Gaster, M., Vortex shedding from slender cones at low Reynolds numbers, J. Fluid Mech., Vol. 38, Part 3, pp. 565-576 (1969)

22   Van Atta, C. W. and Gharib, M., Ordered and chaotic vortex streets behind circular cylinders at low Reynolds numbers, J. Fluid Mech., Vol. 174, pp. 113-133 (1987)

23   Bloor, S., The transition to turbulence in the wake of a circular cylinder, J. Fluid Mech., Vol. 19, Part 2, pp. 290-304 (1964)

24   Wei, T. and Smith, C. R., Secondary vortices in the wake of circular cylinders, J. Fluid Mech., Vol. 169, pp. 513-533 (1986)

25   Blevins, R., The effects of sound on vortex shedding from cylinders, J. Fluid Mech., Vol. 161, pp. 217-237 (1985)

26 Berger, E. and Wille, R., Periodic flow phenomena, Annual Review of Fluid Mechanics, Vol. 4, pp. 313-340 (1972)

27 Farell, C., Flow around fixed circular cylinders: fluctuating loads, J. Engng. Mech. Div. ASCE, Vol. 107, No. EM3, pp. 565-588 (1981)

28 Zdravkovich, M. M., Discussion on [27], J. Engng. Mech. Div. ASCE, Vol. 108, No. EM3, pp. 567-569 (1982)

29 Fleischmann, S. T. and Sallet, D. W., Vortex shedding from cylinders and the resulting unsteady forces and flow phenomenon, Part 1, Shock and Vibration Digest, Vol. 13, No. 11, pp. 9-22 (1981)

30 Norberg, C. and Sunden, B., Turbulence and Reynolds number effects on the flow and fluid forces on a single tube in cross flow, to appear in Journal of Fluids and Structures (1987)

31 Norberg, C., Interaction between freestream turbulence and vortex shedding for a single tube in cross-flow, Journal of Wind Engineering and Industrial Aerodynamics, Vol. 23, pp. 501-514 (1986)

32 Ljungkrona, L. and Mitsner, A., Studium av strömningen kring två cylindrar i tandemarrangement, M.Sc. thesis Dept. Applied Thermodynamics and Fluid Mechanics, Chalmers Univ., Gothenburg (1985) (in Swedish)

33 Blake, W. K., Mechanics of Flow-Induced Sound and Vibration, Vol. 1, Academic Press (1986)

34 Bishop, R. E. D. and Hassan, A. Y., The lift and drag forces on a circular cylinder in a flowing fluid, Proc. Roy. Soc. (London) Ser. A, Vol. 277, pp. 32-50 (1964)

35 Camichel, C., Dupin, P. and Teissié-Solier, M., Sur l'application de la loi de similitude aux périodes de formation des tourbillons alternés de Bénard-Karman, Acad. Sci. Comptes Rendus, Vol. 185, pp. 1556-1559 (1927)

36 Nishioka, M. and Sato, H., Measurements of velocity distributions in the wake of a circular cylinder at low Reynolds numbers, J. Fluid Mech., Vol. 65, Part 1, pp. 97-112 (1974)

37 Kohan, S. and Schwarz, W. H., Low speed calibration formula for vortex shedding from cylinders, Physics of Fluids, Vol. 16, No. 9, pp. 1528-1529 (1973)

38 Friehe, C. A., Vortex shedding from cylinders at low Reynolds numbers, J. Fluid Mech., Vol. 100, Part 2, pp. 237-241 (1980)

39 Taneda, S., Experimental investigation of the wakes behind cylinders and plates at low Reynolds numbers, J. Phys. Soc. Japan, Vol. 11, No. 3, pp. 302-307 (1956)

40 Gaster, M., Vortex shedding from circular cylinders at low Reynolds numbers, J. Fluid Mech., Vol. 46, Part 4, pp. 749-756 (1971)

41 Tritton, D. J., A note on vortex streets behind circular cylinders at low Reynolds numbers, J. Fluid Mech., Vol. 45, Part 1, pp. 203-208 (1971)

42 Newhouse, S., Ruelle, D. and Takens, F., Occurrence of strange axiom A attractors near quasiperiodic flow on T^m, m≥3, Commun. Phys., Vol. 64, pp. 35-40 (1978)

43 Sirovich, L., The Karman vortex trail and flow behind a circular cylinder, Physics of Fluids, Vol. 28, No. 9, pp. 2723-2726 (1985)

44 Hussain, A. K. M. F. and Ramjee, V., Periodic wake behind a circular cylinder at low Reynolds numbers, Aeronautical Quarterly, Vol. 27, No. 2, pp. 123-142 (1976)

45 Berger, E., Unterdrückung der laminaren Wirbelströmung und des Turbulenzeinsatzes der Kármánschen Wirbelstrasse im Nachlauf eines schwingenden Zylinders bei kleinen Reynoldszahlen, Jahrbuch Wiss. Ges. Luftfahrt und Raumfahrt, pp. 164-172 (1964)

46 Hama, F. R., Three-dimensional vortex pattern behind a circular cylinder, J. Aeronautical Sci., Vol. 24, pp. 156-158 (1957)

47 Gerrard, J. H., The mechanics of the formation region of vortices behind bluff bodies, J. Fluid Mech., Vol. 25, Part 2, pp. 401-413 (1966)

48 Bearman, P. W., On vortex shedding from a circular cylinder in the critical regime, J. Fluid Mech., Vol. 37, Part 3, pp. 577-585 (1969)

49 Sonneville, P., Étude de la structure tridimensionelle des écoulements d'un cylindre circulaire, Bulletin de la Direction des Etudes et Recherche Sér. A, Electricité de France, Vol. 3, (1976)

50 Schlichting, H., Boundary Layer Theory, 7th Ed., McGraw-Hill (1979)

51 Unal, M. F. and Rockwell, D., The role of shear layer stability in vortex shedding from cylinders, Physics of Fluids, Vol. 27, No. 11, pp. 2598-2599 (1984)

52 Michalke, A., On spatially growing disturbances in an inviscid shear layer, J. Fluid Mech., Vol. 23, Part 2, pp. 371-383 (1965)

53 Maekawa, T. and Mizuno, S., Flow around the separation point and in the near-wake of a circular cylinder, Physics of Fluids Supplement, pp. S184-S186 (1967)

54 Peterka, J. A. and Richardson, P. D., Effects of sound on separated flows, J. Fluid Mech., Vol. 37, Part 2, pp. 265-287 (1969)

55 Yamanaka, G., Imaichi, K. and Adachi, T., The influence of acoustic disturbances on the mechanics in the shear layer behind a circular cylinder in air flow, DISA Information No. 14, pp. 37-44 (1973)

56   Hama, F. R., Progressive deformation of a perturbed line vortex filament, Physics of Fluids, Vol. 6, No. 4, pp. 526-534 (1963)

57   Braza, M., Chassaing, P. and Ha Minh, H., Numerical study and physical analysis of the pressure and velocity fields in the near wake of a circular cylinder, J. Fluid Mech., Vol. 165, pp. 79-130 (1986)

58   Goldstein, R. J., Fluid Mechanics Measurements, Hemisphere (1985)

59   Schiller, L. and Linke, W., Druck- und Reibungwiderstand des Zylinders bei Reynoldsschen Zahlen 5000 bis 40000, Zeitschrift für Flugtech. Motorluft., Vol. 24, Nr. 7, pp. 193-198 (1933)

60   Allen, H. J. and Vincenti, W. G., Wall interference in a two- dimensional-flow wind tunnel with consideration of the effect of compressibility, NACA Report No. 782 (1944)

61   Roshko, A., A new hodograph for free streamline theory, NACA TN 3168 (1954)

62   Roshko, A., On the wake and drag of bluff bodies, J. Aero. Sci., Vol. 22, No. 2, pp. 124-132 (1955)

63   Bloor, S. and Gerrard, J. H., Measurements on the turbulent vortices in a cylinder wake, Proc. Roy. Soc. (London) Ser. A, Vol. 294, pp. 319-342 (1966)

64   Peltzer, R. D., The effect of upstream shear and surface roughness on the vortex shedding patterns and pressure distributions around a circular cylinder in transitional Reynolds number flows, M.Sc. thesis, VPI & SU (1980)

65   Woo, H. G. C., Cermak, J. E. and Peterka, J. A., Experiments on vortex shedding from stationary and oscillating cables in a linear shear flow, Final report on contract N68305-78-C-0055 for the Naval Civil Engineering Laboratory, Colorado State University (1981)

66   Gerrard, J. H., Experimental investigation of separated boundary layer undergoing transition to turbulence, Physics of Fluids Supplement, pp. S98-S100 (1967)

67   Leehey, P. and Hanson, C. E., Aeolian tones associated with resonant vibration, J. Sound Vibr., Vol. 13, No. 4, pp. 465-483 (1971)

68   Prendergast, V., Measurement of two-point correlations of the surface pressure on a circular cylinder, University of Toronto, UTIAS Tech. Note 23 (1958)

69   el-Baroudi, M. Y., Measurement of two-point correlations of velocity near a cylinder shedding a Karman vortex street, University of Toronto, UTIAS Tech. Note 31 (1960)

70   Hinze, J. O., Turbulence, 2nd Edition, McGraw-Hill (1975)

71   Kacker, S. C., Pennington, B. and Hill, R. S., Fluctuating lift coefficient for a circular cylinder in cross flow, J. Mech. Engng. Sci., Vol. 16, No. 4, pp. 215-224 (1974)

72   Bruun, H. H. and Davies, P. O. A. L., An experimental investigation of the unsteady pressure forces on a circular cylinder in a turbulent cross flow, J. Sound Vibr., Vol. 40 No. 4, pp. 535-559 (1975)

73   West, G. S. and Apelt, C. J., The effects of tunnel blockage and aspect ratio on the mean flow past a circular cylinder with Reynolds numbers between 10^4 and 10^5, J. Fluid Mech., Vol. 114, pp. 361-377 (1982)

74   Thom, A., An investigation of fluid flow in two dimensions, ARC Reports and Memoranda No. 1194 (1928)

75   Thom, A., The flow past circular cylinders at low speeds, Proc. Roy. Soc. (London) Ser. A, Vol. 141, pp. 651-669 (1933)

76   Bearman, P. W. and Morel, T., Effect of free stream turbulence on flow around bluff bodies, Progr. Aero. Sci., Vol. 20, pp. 97-123 (1983)

77   Almosnino, D. and McAlister, K. W., Water-tunnel study of transition flow around circular cylinders, NASA TM 85879 (1984)

78   Schewe, G., On the force fluctuations acting on a circular cylinder in crossflow from subcritical up to transcritical Reynolds numbers, J. Fluid Mech., Vol. 133, pp. 265-285 (1983)

79   Schewe, G., Sensitivity of transition phenomena to small perturbations in flow round a circular cylinder, J. Fluid Mech., Vol. 172, pp. 33-46 (1986)

APPENDIX

DATA POINTS COMPILED IN FIG. 3 (INCLUDING FLOW REGIMES)

Abbreviations for flow regimes:
 ST - Stable
 TR - Transition
 LS - Lower subcritical
 US - Upper subcritical
 C1 - Precritical
 C2 - Paracritical

Notations:
 TU - freestream turbulence intensity
 U_o - freestream velocity
 D - cylinder diameter
 ν - kinematic viscosity
 f_S - vortex shedding frequency
 Δf_S - bandwidth of f_S (-3 dB)

1^O. TU = 0.1%

1a) D = 0.251 mm (35 points)

U_oD/ν	f_SD/U_o	$\Delta f_S/ f_S$ [%]	Regime
47.7	0.1166	0.25	ST
48.9	0.1205	0.15	”
50.0	0.1233	0.14	”
51.2	0.1251	0.16	”
52.8	0.1267	0.56	”
54.2	0.1279	0.20	”
55.3	0.1298	0.45	”
56.8	0.1315	0.16	”
58.1	0.1325	0.15	”
60.4	0.1356	0.11	”
62.9	0.1390	0.24	”
65.4	0.1410	0.48	”
69.2	0.1445	0.42	”
73.0	0.1476	0.13	”
79.3	0.1531	0.10	”
85.5	0.1541	0.19	”
92.4	0.1613	0.16	”
98.8	0.1647	1.01	”
104.9	0.1680	0.84	”
118.1	0.1734	1.00	”
130.9	0.1783	0.11	”
143.7	0.1784	0.19	”
156.7	0.1800	0.42	TR
161.8	0.1824	0.65	”
164.2	0.1798	2.08	”
169.8	0.1812	4.30	”
189.5	0.1820	1.77	”
202.0	0.1841	1.71	”
234.1	0.1913	3.06	”
259.9	0.2019	2.90	”
285.7	0.2033	0.62	LS
311.5	0.2041	0.44	”
343.2	0.2046	0.36	”
375.0	0.2051	0.40	”
413.3	0.2056	0.42	”

1b) D = 0.503 mm (22 points)

U_oD/ν	f_SD/U_o	$\Delta f_S/ f_S$ [%]	Regime
48.2	0.1163	0.40	ST
52.8	0.1246	0.70	”
60.6	0.1348	0.32	”
67.3	0.1407	0.13	”
77.5	0.1512	0.38	”
88.0	0.1582	0.11	”
101.0	0.1657	0.11	”
113.8	0.1718	0.16	”
128.4	0.1785	0.18	”
145.8	0.1776	0.12	”
156.5	0.1793	0.42	TR
161.4	0.1790	0.63	”
184.3	0.1810	1.77	”
222.5	0.1876	1.53	”
261.9	0.2043	0.67	LS
313.5	0.2046	0.38	”
365.3	0.2056	0.35	”
430.0	0.2069	0.21	”
494.2	0.2081	0.27	”
571.5	0.2094	0.44	”
648.4	0.2103	0.19	”
750.6	0.2111	0.30	”

1c) D = 2.00 mm (21 points)

U_oD/ν	f_SD/U_o	$\Delta f_S/f_S$ [%]	Regime
235.3	0.1922	3.73	TR
288.1	0.2024	0.27	LS
340.2	0.2034	0.46	,,
389.9	0.2034	0.30	,,
440.2	0.2054	0.29	,,
494.2	0.2065	0.46	,,
543.0	0.2080	0.23	,,
593.7	0.2087	0.38	,,
645.6	0.2096	0.33	,,
744.8	0.2112	0.29	,,
846.3	0.2120	0.28	,,
1039.4	0.2128	0.21	,,
1238.4	0.2139	0.22	,,
1496.7	0.2140	0.35	,,
1747.8	0.2138	0.17	,,
2002.0	0.2133	0.27	,,
2252.9	0.2134	0.21	,,
2561.0	0.2132	0.35	,,
2864.1	0.2130	0.25	,,
3167.5	0.2127	0.29	,,
3480.1	0.2123	0.25	,,

1d) D = 3.99 mm (16 points)

U_oD/ν	f_SD/U_o	$\Delta f_S/f_S$ [%]	Regime
1066.1	0.2134	0.30	LS
1271.2	0.2129	0.16	,,
1469.0	0.2135	0.26	,,
1872.4	0.2130	0.32	,,
2279.7	0.2125	0.34	,,
2684.3	0.2123	0.23	,,
3198.0	0.2115	0.34	,,
3704.6	0.2108	0.25	,,
4211.1	0.2104	0.21	,,
4724.6	0.2097	0.32	,,
5328.1	0.2086	0.48	US
5935.4	0.2072	0.87	,,
6545.4	0.2059	1.59	,,
7165.1	0.2044	2.25	,,
7995.3	0.2018	1.34	,,
8856.0	0.2006	1.28	,,

1e) D = 5.98 mm (20 points)

U_oD/ν	f_SD/U_o	$\Delta f_S/f_S$ [%]	Regime
2181.1	0.2136	0.35	LS
2482.4	0.2138	0.43	,,
2992.7	0.2125	0.50	,,
3400.9	0.2127	0.41	,,
4006.8	0.2124	0.26	,,
4312.7	0.2122	0.29	,,
4620.5	0.2118	0.34	,,
4926.1	0.2114	0.35	,,
5224.2	0.2111	0.38	US
5524.1	0.2108	0.40	,,
5820.4	0.2102	0.60	,,
6128.3	0.2091	0.65	,,
6435.3	0.2082	0.98	,,
6744.7	0.2072	1.24	,,
7363.9	0.2055	1.57	,,
7986.6	0.2043	1.71	,,
8616.4	0.2036	2.29	,,
9547.1	0.2022	1.55	,,
10462.6	0.2014	1.82	,,
11686.4	0.1995	1.04	,,

1f) D = 9.99 mm (19 points)

U_oD/ν	f_SD/U_o	$\Delta f_S/f_S$ [%]	Regime
3689.9	0.2115	0.60	LS
4182.5	0.2116	0.55	,,
5199.9	0.2106	0.61	US
6213.7	0.2101	0.93	,,
7235.3	0.2077	1.86	"
7759.4	0.2066	2.54	"
8245.6	0.2040	1.15	"
8741.5	0.2034	1.32	"
9222.2	0.2023	1.25	"
9785.6	0.2013	1.81	"
10484.2	0.2002	1.80	"
11745.6	0.1984	1.83	"
13242.2	0.1975	2.02	"
14737.9	0.1966	2.11	"
16227.6	0.1959	2.08	"
17750.4	0.1957	2.49	"
19764.4	0.1948	1.83	"
21819.5	0.1940	1.50	"
24004.4	0.1933	2.24	"

1g) D = 41.0 mm (22 points)

U_oD/ν	f_SD/U_o	$\Delta f_S/f_S$ [%]	Regime
10654.0	0.2006	3.30	US
12723.6	0.1987	2.90	”
14783.1	0.1966	3.00	“
16768.4	0.1959	2.70	“
20853.3	0.1946	2.90	“
24959.7	0.1940	3.00	“
29019.6	0.1939	4.20	“
33165.9	0.1915	5.30	“
37221.7	0.1916	5.30	“
41278.1	0.1906	4.30	“
45304.5	0.1895	3.50	“
49438.9	0.1893	5.10	“
53514.0	0.1887	3.70	“
57551.4	0.1889	4.60	“
61603.2	0.1882	4.70	“
65715.7	0.1876	5.80	“
69897.4	0.1875	3.80	“
76182.5	0.1879	3.70	“
80681.9	0.1869	4.10	“
84595.0	0.1868	4.90	“
88571.2	0.1861	5.50	“
92506.2	0.1861	4.20	“

1h) D = 120.0 mm (13 points)
Note: freestream velocity U_o blockage
corrected 5.8%

U_oD/ν	f_SD/U_o	$\Delta f_S/f_S$ [%]	Regime
61747.1	0.1894	7.30	US
67418.8	0.1880	7.50	”
79599.9	0.1882	7.40	“
91560.1	0.1870	6.40	“
103717.8	0.1870	5.50	“
121445.3	0.1868	7.60	“
139350.5	0.1873	6.90	“
163026.7	0.1873	5.70	“
186616.7	0.1880	5.10	“
210348.2	0.1901	4.10	C1
240623.2	0.1940	2.60	“
271612.9	0.1999	2.40	“
303163.9	0.2083	1.90	“

2^O. TU = 1.4%

2a) D = 0.251 mm (16 points)

U_oD/ν	f_SD/U_o	$\Delta f_S/f_S$ [%]	Regime
47.4	0.1174	2.29	ST
51.3	0.1239	3.24	"
58.4	0.1320	2.77	"
68.3	0.1444	2.36	"
84.2	0.1547	2.56	"
103.8	0.1662	2.40	"
125.8	0.1737	3.20	"
141.9	0.1784	2.89	"
149.7	0.1808	2.81	"
158.0	0.1826	3.72	TR
173.8	0.1813	4.27	"
197.6	0.1843	3.22	"
221.2	0.1878	3.78	"
245.0	0.1988	5.73	"
276.9	0.2030	2.96	LS
308.6	0.2037	2.38	"

2b) D = 0.503 mm (14 points)

U_oD/ν	f_SD/U_o	$\Delta f_S/f_S$ [%]	Regime
48.3	0.1179	2.38	ST
57.2	0.1292	2.39	"
75.8	0.1488	1.77	"
95.1	0.1630	1.94	"
122.9	0.1754	1.76	"
151.9	0.1867	1.88	"
207.8	0.1837	2.60	TR
267.5	0.2045	1.34	LS
315.5	0.2049	1.07	"
363.7	0.2058	1.46	"
411.8	0.2068	1.20	"
475.2	0.2082	1.45	"
554.6	0.2097	1.44	"
633.3	0.2106	1.12	"

2c) D = 2.00 mm (19 points)

U_oD/ν	f_SD/U_o	$\Delta f_S/f_S$ [%]	Regime
548.6	0.2078	0.76	LS
608.0	0.2088	1.14	"
667.2	0.2094	0.98	"
729.5	0.2103	0.89	"
869.3	0.2124	0.67	"
938.4	0.2122	0.60	"
1002.8	0.2127	0.65	"
1064.2	0.2135	0.76	"
1127.4	0.2135	0.48	"
1190.7	0.2132	0.50	"
1320.2	0.2129	0.49	"
1447.7	0.2128	0.64	"
1640.5	0.2122	0.63	"
1831.4	0.2118	0.70	"
2022.8	0.2114	0.57	"
2223.1	0.2111	0.55	"
2484.3	0.2112	0.33	"
2964.6	0.2105	0.42	"
3193.2	0.2103	0.63	"

2d) D = 3.99 mm (16 points)

U_oD/ν	f_SD/U_o	$\Delta f_S/f_S$ [%]	Regime
1889.0	0.2117	0.39	LS
2020.5	0.2112	0.51	"
2147.3	0.2110	0.53	"
2401.0	0.2107	0.51	"
2658.6	0.2101	0.56	"
2980.6	0.2093	0.43	"
3300.6	0.2089	0.36	"
3683.2	0.2085	0.46	"
4081.1	0.2077	0.71	US
4620.0	0.2069	0.61	"
5131.0	0.2057	0.95	"
5621.4	0.2044	1.24	"
6221.6	0.2031	1.50	"
6801.1	0.2018	1.96	"
7430.2	0.2015	1.03	"
8085.2	0.2001	1.75	"

2e) D = 5.98 mm (14 points)

U_oD/ν	f_SD/U_o	$\Delta f_S/f_S$ [%]	Regime
3012.9	0.2088	0.58	LS
3213.3	0.2082	0.43	"
3591.4	0.2082	0.36	"
3969.0	0.2082	0.39	"
4377.6	0.2065	0.56	US
4756.1	0.2054	0.71	"
5126.2	0.2046	0.85	"
5683.6	0.2031	1.15	"
6262.3	0.2019	1.55	"
6802.2	0.2011	1.15	"
7531.2	0.1996	1.24	"

U$_o$D/ν	f$_S$D/U$_o$	Δf$_S$/ f$_S$ [%]	Regime
8263.2	0.1983	1.13	"
9000.7	0.1981	1.22	"
9770.8	0.1976	1.57	"

2f) D = 9.99 mm (15 points)

U$_o$D/ν	f$_S$D/U$_o$	Δf$_S$/ f$_S$ [%]	Regime
3229.0	0.2080	1.00	LS
3887.4	0.2080	1.38	"
5090.4	0.2075	0.87	US
5902.2	0.2048	1.52	"
6731.3	0.2021	1.16	"
7717.2	0.1999	1.54	"
8634.2	0.1989	1.56	"
9882.0	0.1974	1.88	"
11123.1	0.1967	1.22	"
12336.7	0.1964	1.07	"
13553.4	0.1958	1.75	"
15071.1	0.1949	1.57	"
16583.9	0.1947	1.09	"
17813.4	0.1944	1.45	"
19763.3	0.1934	1.72	"

2g) D = 41.0 mm (17 points)

U$_o$D/ν	f$_S$D/U$_o$	Δf$_S$/ f$_S$ [%]	Regime
18006.8	0.1940	2.40	US
20620.8	0.1933	2.60	"
23276.5	0.1926	2.40	"
25831.8	0.1917	2.70	"
29101.3	0.1912	2.40	"
32404.1	0.1898	3.00	"
35689.6	0.1892	2.60	"
39123.2	0.1895	3.30	"
42554.4	0.1885	2.90	"
45776.2	0.1887	4.10	"
49511.6	0.1883	2.50	"
53292.9	0.1880	3.70	"
60747.2	0.1877	3.30	"
65793.9	0.1877	4.10	"
70899.0	0.1876	4.00	"
75741.0	0.1880	3.00	"
81027.6	0.1876	4.10	"

2h) D = 120.0 mm (14 points)
Note: freestream velocity U$_o$ blockage corrected 5.8%

U$_o$D/ν	f$_S$D/U$_o$	Δf$_S$/ f$_S$ [%]	Regime
81617.1	0.1875	3.80	US
93340.9	0.1875	3.30	"
105363.4	0.1875	3.60	C1
117977.9	0.1876	3.70	"
129933.4	0.1889	3.90	"
141567.2	0.1920	4.60	"
153061.0	0.1934	13.20	"
164454.2	0.1948	36.20	"
175805.7	0.2088	47.40	"
187368.7	0.2233	62.80	C2
198754.9	0.2389	60.0	"
210449.2	0.2585	42.00	"
222694.7	0.2800	30.80	"
236981.0	0.3189	19.50	"